Geophys. J. Int. (2003) **154,** 233–252

Magnetostratigraphy of Tertiary sediments from the Hoh Xil Basin: implications for the Cenozoic tectonic history of the Tibetan Plateau

Zhifei Liu,[1,3] Xixi Zhao,[2] Chengshan Wang,[3] Shun Liu[3] and Haisheng Yi[3]

[1] *Laboratory of Marine Geology, Tongji University, Shanghai* 200092, *China*
[2] *Institute of Tectonics and Earth Sciences Department, University of California, Santa Cruz,* CA 95064, *USA. E-mail: xzhao@es.ucsc.edu*
[3] *Institute of Sedimentary Geology, Chengdu University of Technology, Chengdu* 610059, *China*

Accepted 2002 November 1. Received 2002 October 28; in original form 2000 June 20

SUMMARY

We conducted an integrated palaeomagnetic and stratigraphic study on a 5452.8 m thick sedimentary sequence of the Hoh Xil Basin in northern Qinghai-Tibet Plateau to obtain a chronostratigraphic framework for these sediments. A total of 966 individual oriented palaeomagnetic samples (spaced at stratigraphic intervals) were collected from six measured sections in the Hoh Xil Basin. Magnetic directions in these samples were obtained by progressive thermal (mainly) and alternating-field demagnetization experiments. Most samples exhibit two components of magnetization. The lower unblocking temperature component is an overprint resembling the present-day geocentric axial dipole field direction at the sampling locality. The most stable, characteristic remanence (ChRM) appears to be an early chemical remanent magnetization residing mainly in haematite. The positive results of fold and reversal tests indicate that the ChRM is a record of the palaeomagnetic field close to the time of formation of these sediments. Further evidence for the magnetization of these sediments acquired close to their time of deposition is the fact that patterns of magnetic reversals can be matched with the established polarity timescale. On the basis of the distinct interval of magnetic reversal zones and biostratigraphic datums, 13 magnetozones can be recognized at the Hoh Xil Basin that range from chrons C11 to C23 (30.1–51.0 Ma). The age of the Fenghuoshan Group is palaeomagnetically dated as 51–31 Ma (Early Eocene–Middle Early Oligocene), and the age of the Yaxicuo Group is between 31 and 30 Ma (Middle Early Oligocene–Late Early Oligocene). The new palaeomagnetic data from the Fenghuoshan Group suggest that it has undergone no significant rotation since the Oligocene. In contrast, declination data from the Yaxicuo Group in Wudaoliang area imply a vertical-axis clockwise rotation ($29.1^\circ \pm 8.5^\circ$) since the Late Oligocene. The Tertiary palaeomagnetic pole position of the Hoh Xil Basin implies a significant northward convergence of the Hoh Xil Basin ($\sim$1600 km) with respect to Eurasia (Siberia) since Early Eocene–Late Oligocene time. Our results are consistent with the pattern of disturbingly low palaeolatitudes derived from a large number of high-quality palaeomagnetic studies of Tertiary rocks from sites that reach all the way from eastern China to Kyrgyzstan. Future work is needed to separate the influences of sedimentary inclination shallowing and tectonic shortening.

Key words: central Asia, magnetostratigraphy, Tibet, uplift.

1 INTRODUCTION

The collision between India and Asia has forcefully raised the Tibetan plateau (Argand 1924; Molnar & Tapponnier 1975), which is the highest and most extensive plateau on Earth today. It is also well known as the 'roof' of the world and the 'third pole' of the Earth. Although earth scientists do not debate the current distribution of topography in the Tibetan plateau, the manner in which it evolved both prior to and since the onset of collision remains a lively topic and continues to draw world attention (Yin & Harrison 2000). Consequently, the Tibetan plateau has become the principal natural laboratory for studying continent–continent collision and the uplift history of the continental lithosphere. This region has challenged structural geologists, petrologists, geophysicists and geochronologists alike. Because of its high elevation and large size, the uplift of the plateau has also been thought to play a major role in the Pleistocene global cooling (Ruddiman & Kutzbach 1991; Kutzbach *et al.* 1993; Ruddiman *et al.* 1997; Harrison *et al.* 1998) and the Asian Monsoons (An *et al.* 2001).

While the bounding regions of the plateau, defined by active thrust and strike-slip faults, have been extensively studied for the ongoing tectonic activity, the geological history of the Tibetan interior

has not yet been convincingly established, especially for the early uplift history of the plateau (Ruddiman 1998). The hinterland of the Tibetan plateau, a region that contains erosional products of Tibetan uplift and preserves an important record of its tectonic evolution, receives much less attention because of its harsh conditions for fieldwork. The Hoh Xil basin, with an area of 101 000 km^2 and an average elevation of over 5000 m, is the largest sedimentary basin in the region (Fig. 1). A geological survey of the basin was only conducted relative recently (Coward *et al.* 1990; Yi *et al.* 1990; BGMRQ 1991; Zhang & Zheng 1994). The interpretation of the geology of this basin has led to a variety of estimates of the age for the basin formation, ranging from the Palaeocene/Eocene (Yi *et al.* 1990) to the Late Cretaceous (BGMRQ 1991) the Early Cretaceous (Zhang & Zheng 1994). Two of the previous international geotraverses of the region also reported preliminary palaeomagnetic data from a single sampling locality in Fenghuoshan area (Lin & Watts 1988; Halim *et al.* 1998). However, results are few and also subject to conflicting interpretations (Halim *et al.* 1998). Thus, although these results constitute a beginning and provide a reference for comparison and refinement, they do not constrain the age of the basin formation. Interest has increasingly focused on whether the Hoh Xil Basin was formed during the Cretaceous or the Tertiary. The lack of agreement concerning the age of the basin hinders our understanding of the regional tectonic evolution and palaeogeography.

Magnetic polarity stratigraphy is a tool of great promise for precise temporal correlation and accurate dating in sediments, and can be most helpful in discriminating between these age estimates. Because the time between successive reversals is a random variable following very nearly a Poisson distribution (Merrill *et al.* 1996), the pattern of thicknesses of several magnetozones in each part of a steadily deposited section is a distinctive fingerprint (analogous to the zebra-stripe bar codes used in libraries and supermarkets) that can be correlated between distant sections and matched to the established geomagnetic polarity timescale (GPTS). This scale, which has been established independently by radiometric dating and refined by cross-checking among multiple records, provides dates for reversals that occurred during the last 150 Myr of the Earth's history (e.g. Harland *et al.* 1990; Cande & Kent 1992, 1995; Berggren *et al.* 1995; Channell *et al.* 1995; Opdyke & Channell 1996). As mentioned, because of the harsh working conditions of the Tibetan plateau, no magnetostratigraphic data are available from the Hoh Xil Basin to help define the ages of the sedimentary sequences.

In this paper, we present new magnetostratigraphic results obtained from sedimentary sessions at the Hoh Xil Basin in an effort to remedy this situation and to test the hypothesis of whether the basin was formed during the Cretaceous or the Tertiary. We first describe and discuss the palaeomagnetic polarity patterns of the sediments that provided the most readily interpretable data. We subsequently interpret the polarity sequence, based on conjunction with biostratigraphy and the geomagnetic polarity timescale of Cande & Kent (1992, 1995) and present a magnetostratigraphy for these sessions. We then use the magnetostratigraphy to estimate the sediment accumulation rates and the times at which significant changes in these rates occurred. Finally, we estimate tectonic rotations and palaeolatitudes at which the sediments were deposited using the age and average magnetic directions available from the magnetostratigraphy. Such information has importance in evaluating the recent geological and tectonic evolution of the Tibetan plateau.

2 GEOLOGY AND PALAEOMAGNETIC SAMPLING

Situated in the western part of the Baya Har terrain (BT) and the northern part of the Qiangtang terrain (QT), the Hoh Xil Basin is bounded on the north by South Kunlun Suture Zone (SKSZ) and the Kunlun Mountain and on the south by the Kangbataqing fault and the Tanggula Mountain (Fig. 1, inset). The Jinsha River Suture Zone (JRSZ), one of the five continental suture zones on the Tibetan plateau runs through the eastern part of the basin and sharply bends to the south (Fig. 1).

The basement of the Hoh Xil Basin consists of slate, metasandstone and phyllite formed during the Triassic, Permian and Carboniferous (Zhang & Zheng 1994, shown as the pre-Tertiary basement in Fig. 1). The cover strata of the Hoh Xil Basin, with a total sediment pile of 5821.4 m thick, contain the Fenghuoshan and Yaxicuo Groups in the lower part and the Wudaoliang Group in the upper part. The Fenghuoshan Group with 4782.8 m thickness consists of grey-violet sandstone, mudstone/shale and conglomerate, intercalating grey-green Cu-containing sandstone, dark grey bioclastic limestone and grey layering and tubercular gypsolith. The Fenghuoshan Group consists mainly of fluvial and lacustrine facies, with lesser fan-delta facies near the middle part of the group (Liu & Wang 2001). The Yaxicuo Group (670.0 m thick) mainly consists of the alternating red-violet sandstone, mudstone and shale intercalating grey layering and tubercular gypsolith. Satellite images and field observations show that the Fenghuoshan Group contacts conformably with the overlying Yaxicuo Group. The Wudaoliang Group consists mainly of the lake carbonate with some black oil shale (Liu & Wang 1999). It disconformably overlies the Fenghuoshan and Yaxicuo Groups and its age is widely accepted as Early Miocene based on abundant fossils (BGMRQ 1991; Zhang & Zheng 1994). Although several Palaeocene/Eocene fossil assemblages have been found in a bio-limestone bed (20 cm thick) of the Fenghuoshan Group (Yi *et al.* 1990), no fossils or ash layers have been found in the Yaxicuo Group to provide possible age constraints.

To obtain a chronostratigraphic framework for these sediments and to contribute to the answer to the question of formation age for the Hoh Xil Basin, we made palaeomagnetic-sampling expeditions during the summers of 1997 and 1998. A total of 966 individual oriented palaeomagnetic samples (spaced at stratigraphic intervals) were collected from six measured sections in the Hoh Xil Basin. Magnetic polarity stratigraphy sections (GX, YP, GS and SP) of the Fenghuoshan Group were conducted in the Fenghuoshan area (Figs 2 and 3), whereas magnetostratigraphy sections (GG1 and GG2) of the Yaxicuo Group were measured in the Wudaoliang area (Fig. 4). These sections exhibit well-exposed outcrops of red mudstone, sandstone and conglomerate (Table 1). We correlated these sections by the method of parallel movement along the strike of sedimentary strata and were guided both by the satellite images (Fig. 2a) and field mapping.

The structural variations at each area allowed local fold and/or tilt tests to be applied (Table 1). In the Fenghuoshan area, sections of GX, YP and GS are mainly distributed along both limbs of a syncline and section SP is near the core of another syncline to the east (Fig. 3). In the Wudaoliang area, sections of GG1 and GG2 are situated on two limbs of an overturned anticline, respectively (Fig. 4). Both local folding and regional deformation in these two areas occurred between the Eocene and the Early Miocene, as suggested by regional

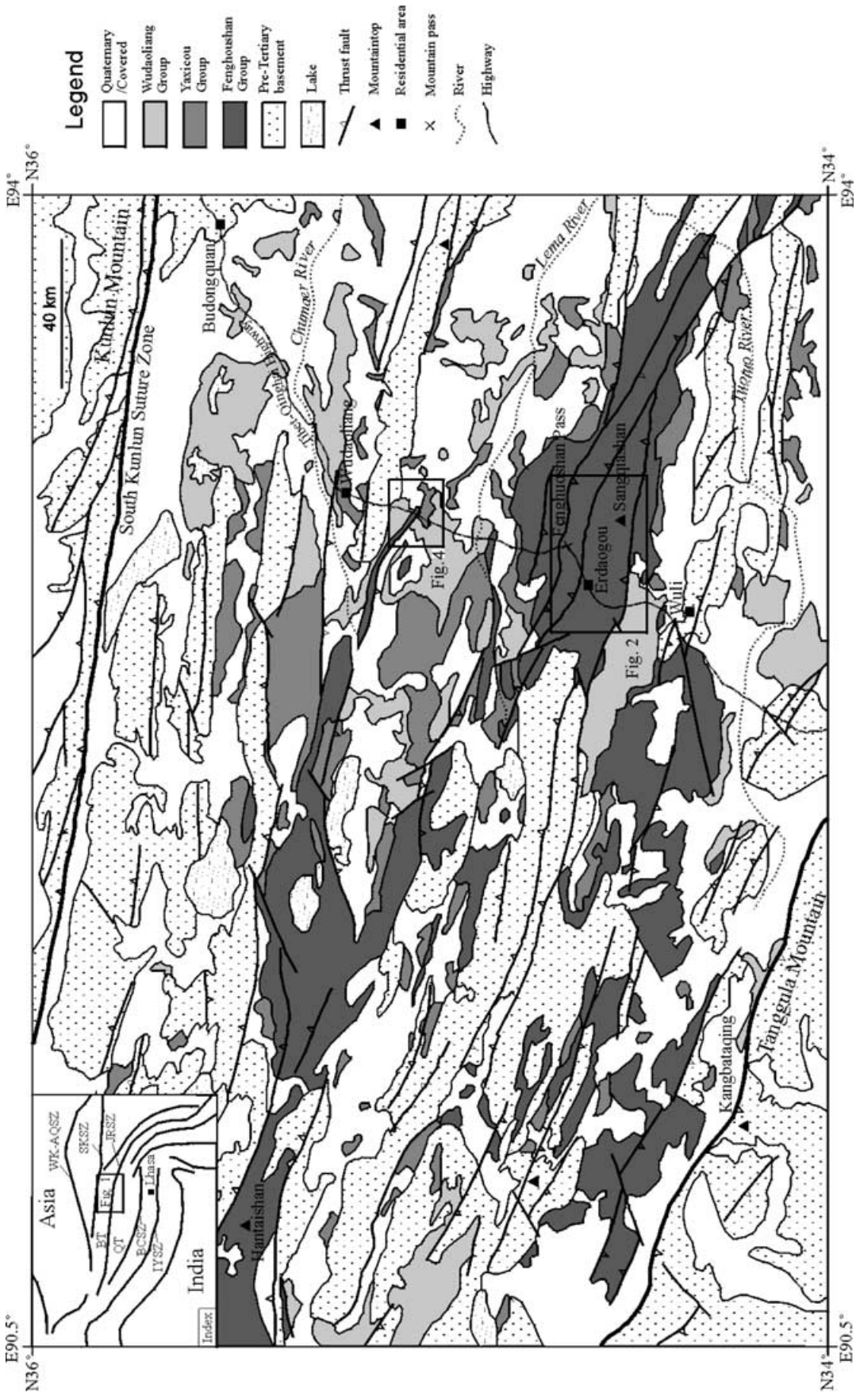

Figure 1. Geological map of the Hoh Xil region, northern Tibet. Pre-Tertiary basement includes slate, metasandstone and phyllite formed in periods of Triassic, Permian and Carboniferous (Modified and simplified from Zhang & Zheng 1994). In Index map: IYSZ, Indus Yarlung Zangbo Suture Zone; BCSZ, Banggong Cuo Suture Zone; JRSZ, Jingsha River Suture Zone; SKSZ, South Kunlun Suture Zone; WK-AQSZ, West Kunlun–Arerjing–Qilian Suture Zone; QT, Qiangtang Terrain; BT, Baya Har Terrain.

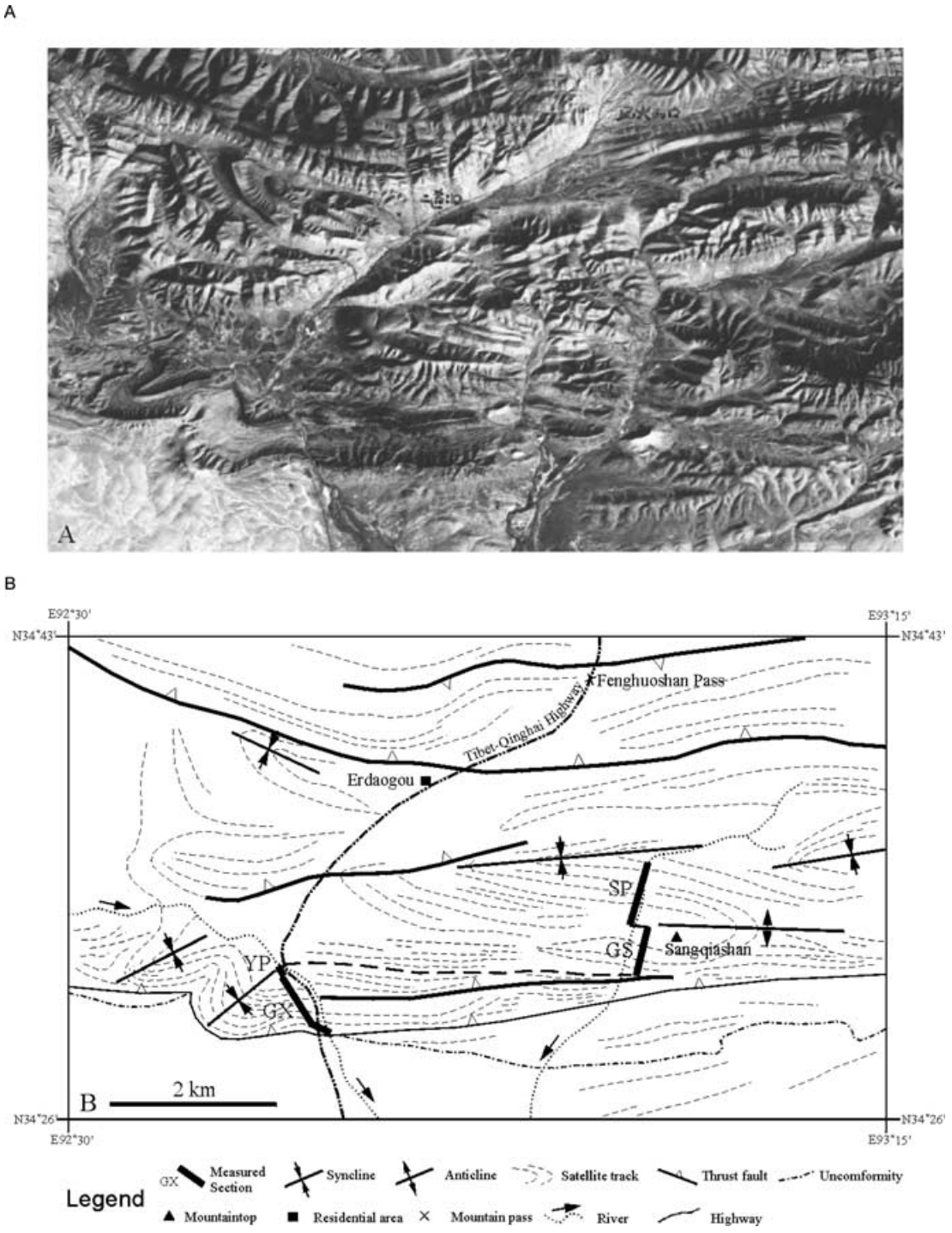

Figure 2. Geological sketch map and satellite image (a) of the Fenghuoshan area in the southeastern Hoh Xil basin, showing tectonic and stratigraphic frames and locations of measured sections of the Fenghuoshan Group (b). See Fig. 1 for the location.

unconformity and by the available Rb-Sr isotopic age (22.3 Ma, million years ago) from an overlying basalt flow in the Zhuolai Lake region (Zhang & Zheng 1994).

Sampling was mainly conducted at grey and red-violet mudstone and sandstone at a thickness span of approximately 10 m for mudstone and of approximately 12 m for sandstone to determine magnetostratigraphy (Fig. 5). Several sites were also collected specifically for rotational analysis, consisting of multiple samples at a stratigraphic level. Sampling followed standard palaeomagnetic practice with *in situ* drilling by a portable gasoline-powered core drill or with hand sampling of well-defined blocks. Orientation was done using both a magnetic compass mounted on an orienting device and a sun compass. The mean difference between the two compass readings was $\pm 1^{\circ}$, in excellent agreement with the local geomagnetic field declination predicted from the 1995 International Geomagnetic Reference Field (IGRF) for the region (IAGA Division V, Working Group 8 1995), indicating that local magnetic anomalies are negligible and averaged out in the mean. An *in situ*

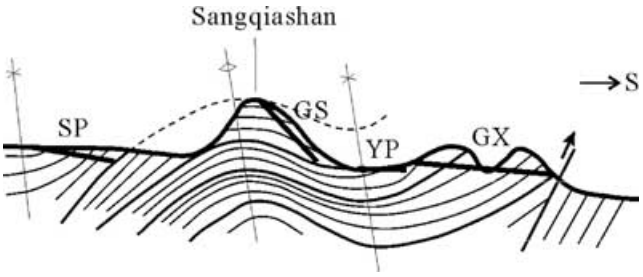

Figure 3. Schematic diagram showing the relationship between sections of GX, YP, GS and SP.

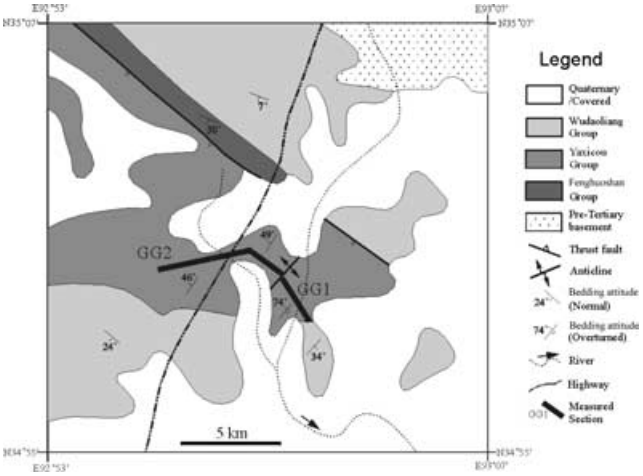

Figure 4. Simplified geological map of the Wudaoliang area in the eastern Hoh Xil basin, indicating locations of measured sections of the Yaxicuo Group. See Fig. 1 for the location.

hand-sampling technique was adopted when the core drill stopped working at the higher elevations. The blocks were oriented using a magnetic compass and were drilled on a horizontal plane in the laboratory. Stratigraphic locations and orientations of each sampling site were carefully recorded during the course of the fieldwork. Samples were trimmed into 2.2 cm long cylinders for subsequent palaeomagnetic analysis.

3 EXPERIMENTAL PROCEDURES AND MAGNETIC DATA ANYALYSIS

All of the experimental work was undertaken in a magnetically shielded room. The samples were subjected to progressive thermal (mainly) and alternating field (AF) demagnetization and measured at each step of treatment by a 2G cryogenic magnetometer at the palaeomagnetic laboratory of the University of California, Santa Cruz (UCSC). Bulk magnetic susceptibility was also measured after every demagnetization step to detect whether chemical changes were affecting the magnetization during progressive heating. Magnetization directions were determined by principal-component analysis (Kirschvink 1980). The distributions of palaeomagnetic directions at each site were calculated using Fisher (1953) statistics and site mean directions of all demagnetized data were derived by giving a unit weighting to each mean sample direction. The analysis of vertical axis rotation employed the technique of Coe *et al.* (1985). A few representative samples were also selected for a set of rock-magnetic measurements to examine their mineralogical characteristics. These rock-magnetic measurements included Curie temperature determinations, acquisition of isothermal remanent magnetization (IRM) and backfield demagnetization of saturation IRM, performed both at UCSC and at the Institute for Rock Magnetism, University of Minnesota.

4 MAGNETIC RESULTS

4.1 General view

Within the six measured sections where magnetostratigraphy can be constructed, there were considerable variations in demagnetization behaviour among the various lithologies. In general, AF demagnetization was less effective in isolating magnetic components. Comparison of thermal and AF demagnetization results from the same site showed that in some cases AF demagnetization failed to remove secondary magnetization adequately. Based on this experience, thermal treatments were applied to the rest of the samples. The commonest features of the thermal demagnetization data can be summarized as follows: a small, soft component of magnetization was easily removed during the initial demagnetization. The directions of the soft component generally cluster near the geocentric axial dipole field (GAD) field direction at the sampling area. Progressive thermal demagnetization to 700°C, however, revealed two other magnetization components. An intermediate unblocking temperature component (ITC) was isolated in most samples by best-fitting lines to demagnetization data between 300 and 500°C. Interestingly, the directions of the ITC in some red sandstones are reversed. This reversed ITC magnetization is compatible with a reversed event prior to the Brunhes (>0.78 Ma) and is incompatible with a Holocene field direction. A very high unblocking temperature component (HTC) was isolated between 625 and 700°C in almost all red sandstone samples. The HTC has both normal and reversed polarities and is interpreted as the characteristic remanent magnetization (ChRM) on the basis of linear trajectories of demagnetization towards the origin and a similar direction from sample to sample. In some samples, the vector endpoints miss the origin and align on a great circle. For these samples, a great circle analysis technique (McFadden & McElhinny 1988) was used to establish the characteristic direction.

Table 1. Palaeomagnetic sampling details of the Hoh Xil basin from this study.

Measured locality (formation) section	Thickness (m)	SLat (°N)	SLong (°E)	*N*	Strike (deg)	Dip (deg)
GG1 Wudaoliang (Yaxicuo)	196.2	34° 59′ 57.″1	93° 00′ 01.″4	16	54–239	82–160
GG2 Wudaoliang (Yaxicuo)	670.0	34° 59′ 55.″1	92° 58′ 45.″0	133	199–252	25–84
SP Sangqiashan (Fenghuoshan)	1447.2	34° 45′ 56.″1	92° 54′ 01.″8	361	270–325	25–82
GS Sangqiashan (Fenghuoshan)	1369.4	34° 45′ 56.″1	92° 54′ 01.″8	170	271–150	9–89
YP Erdaogou (Fenghuoshan)	222.9	34° 33′ 10.″0	92° 40′ 08.″8	47	305–45	22–46
GX Erdaogou (Fenghuoshan)	1740.3	34° 32′ 20.″2	92° 42′ 09.″6	239	277–316	32–90

SLat/SLong: latitude/longitude of sampling locality, *N*, number of samples used in this study.

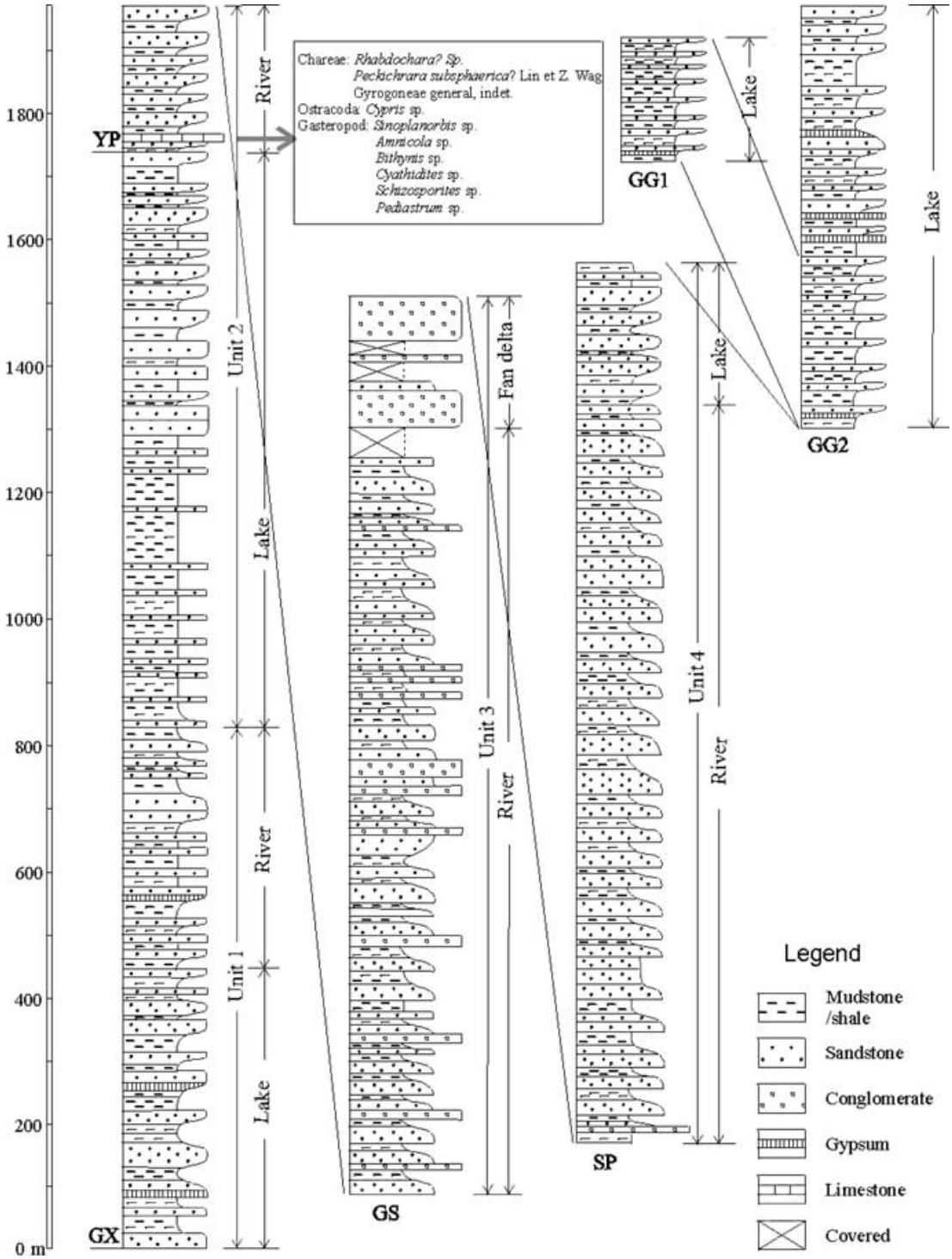

Figure 5. Detailed sedimentary logs of the measured sections showing lithology and sedimentary environments of the Fenghuoshan and Yaxicuo Groups. The scale is at left-hand (all on the same scale). See Figs 2 and 4 for the locations of the sections.

Response of the ChRM to AF and thermal demagnetization suggests that in the majority of samples the ChRM is carried by haematite. We conducted several rock-magnetic analyses on representative samples to further characterize the magnetic minerals and understand their rock-magnetic properties. Results from these experiments all corroborate the demagnetization behaviour and suggest that haematite is the main magnetic carrier in these redbeds. As shown in Fig. 6, the hysteresis loop for a redbed sample displays constricted (wasp-waisted) behaviour, which is typical for the presence of low-coercivity magnetite and high-coercivity haematite (Tauxe *et al.* 1996).

4.2 Sections GG2 and GG1

Sections GG2 and GG1 of the Yaxicuo Group were measured on the two limbs of an overturned anticline in the Wudaoliang area (Fig. 4).

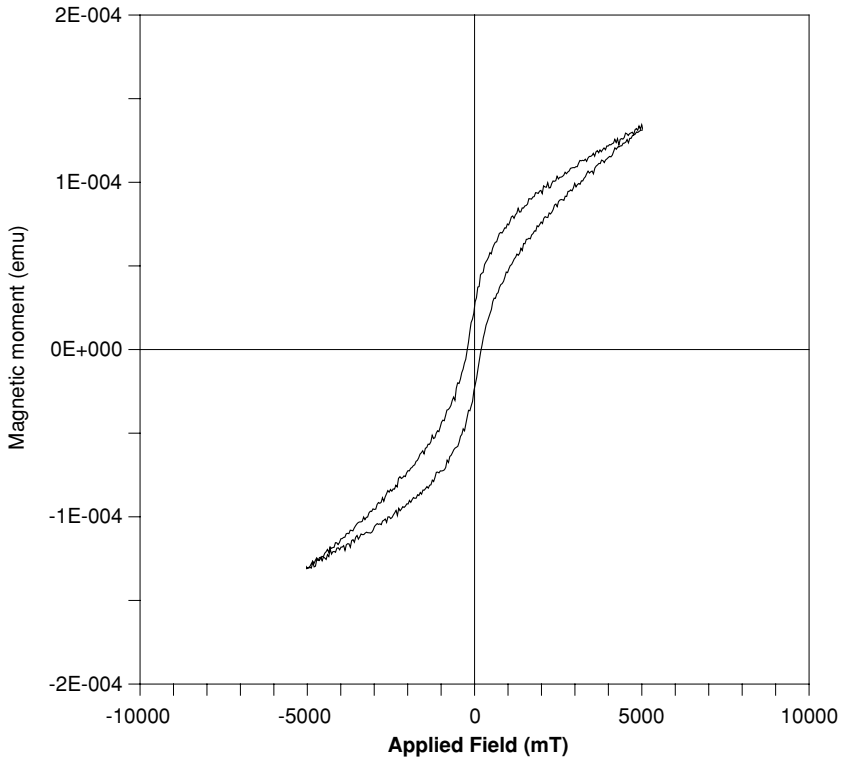

Figure 6. Representative magnetic hysteresis characteristic curve for a redbed sample from stratigraphic level 3584.1 m of SQ section displays constricted loop (wasp-waisted) behaviour, which is typical for the presence of low-coercivity magnetite and high-coercivity haematite. Data are shown corrected for the sample probe only.

A total of 133 red sandstone samples were collected from section GG2, but only 16 samples were obtained from section GG1. The stratigraphic sequence of section GG1 can be correlated with the lower part of section GG2, providing an opportunity to apply the fold test on magnetic components. Each of these 149 samples was subjected to progressive thermal demagnetization to determine the characteristic magnetization.

As shown in Fig. 7(a), demagnetization at temperatures up to 500 °C effectively removed an overprint and isolated a characteristic direction. The ChRM is obtained predominantly in the 600–675 °C interval, showing that haematite is the main carrier of the ChRM. Both normal and reversed polarity directions were obtained (Fig. 8a and Table 2). The overall mean direction for this section is at D (declination) $= 69.5^\circ$, I (inclination) $= 18.6^\circ$, $N = 59$ sites, k (precision parameter of the site mean direction) $= 3.9$ and a_{95} (95 per cent confidence circle of the site mean direction) $= 10.8^\circ$ in geographic coordinates and $D = 37.2^\circ$, $I = 40.8^\circ$, $k = 8.6$, $a_{95} = 6.7^\circ$ in stratigraphic coordinates (Table 2). Using the test of McFadden (1990), the fold test results are positive at more than 95 per cent confidence level. The mean normal and reversed directions (Table 2) are not significantly different from antipodal at the 95 per cent confidence level, affording a positive reversal test (C class reversal test in McFadden & McElhinny 1990).

4.3 Section SP

We sampled a total of 361 red sandstone samples from three sections (sections SP 19, 20 and 21) in the Fenghuoshan area. These sandstone rocks are in the upper part of the Fenghuoshan Group. Stratigraphic and palaeontological studies have indicated a pre-Yaxicuo Group age for these rocks, according to our field studies. We used progressive thermal demagnetization at a minimum of 10 levels to resolve the magnetic components. Most samples from the SP section display rather straightforward demagnetization behaviour, characterized by a single linear trajectory over a broad temperature range after removal of a viscous component and sometimes a second ITC (Fig. 7b). The fact that the magnetization persists to temperature treatments of up to 700 °C indicates that haematite is most probably the carrier of ChRM.

The direction of the final high-temperature component is predominantly reversed polarity, but 16 samples towards the middle part of the section revealed normal polarity (Fig. 8b). The mean normal and reversed directions (Table 2) are not significantly different from antipodal at the 95 per cent confidence level (C class reversal test in McFadden & McElhinny 1990). In contrast to sections GG2 and GG1 of the Yaxicuo Group in the Wudaoliang area described above, which show persistent eastwardly deflected declinations, the ChRM direction for the SP section is directed more northwesterly with intermediate to steep downward inclination. Before tectonic correction, the mean direction is $D = 296.5^\circ$, $I = 59.4^\circ$, $N = 51$ sites, $k = 5.7$, $a_{95} = 9.2^\circ$. After tectonic correction, the mean direction of the ChRM becomes $D = 350.0^\circ$, $I = 37.4^\circ$ with $k = 6.8$ and $a_{95} = 8.3^\circ$. As shown in Table 3, the SCOS value in the unfolded coordinates (4.065) is much less than the critical value at the 99 per cent confidence level (11.746), demonstrating that the fold test for the SP sections is also positive at the 99 per cent confidence level.

4.4 Section GS

We measured section GS in the Sangqiashan area along the stratigraphic strike (Figs 2b and 3). A total of 170 samples were collected from section GS. The demagnetization characteristics varied among

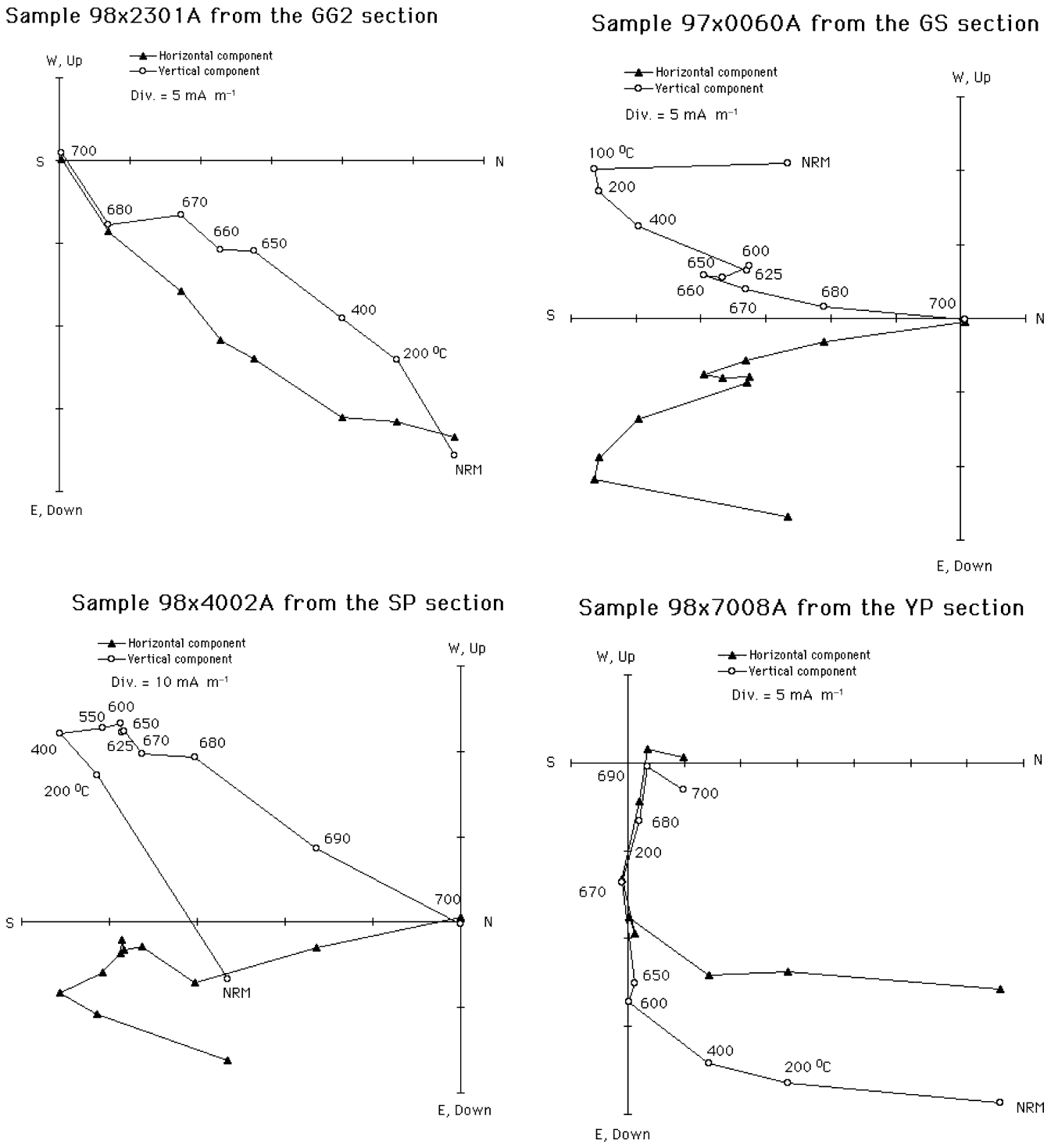

Figure 7. Representative vector endpoint diagrams showing results of thermal demagnetization for samples from the Hoh Xil basin. (a) Sample 98X2301 from the GG2 section; (b) sample 98X4002A from the SP section; (c) sample 97X0060A from the GS section; (d) sample, 98X7008 from the YP section; and (e) sample 97X0030A from the GX section. Directions are plotted in geographic coordinates. Crosses and circles represent the projection of the magnetization vector endpoint on the horizontal and vertical planes, respectively. NRM: natural remanent magnetization. Temperatures shown are in degrees Celsius.

the sampled sites. Although some demagnetization diagrams show erratic behaviour and reveal remagnetization upon thermal treatment in the laboratory, the vast majority of the samples are quite well behaved and reveal two magnetic components (Fig. 7c). The low-temperature component (LTC) is exhibited at low temperatures (200–400 °C) and sometimes persisted until high temperatures (<600 °C). The direction of the LTC fails a fold test at acquired the 95 per cent confidence level, indicating a magnetization after tilting. Nevertheless, the fact that the individual directions for the LTC are always close (if not identical) to the recent field direction at the sampling area, suggesting that this LTC is not only an overprint acquired after folding in recent times, but also indicating that orientation errors are not significant in collecting these samples.

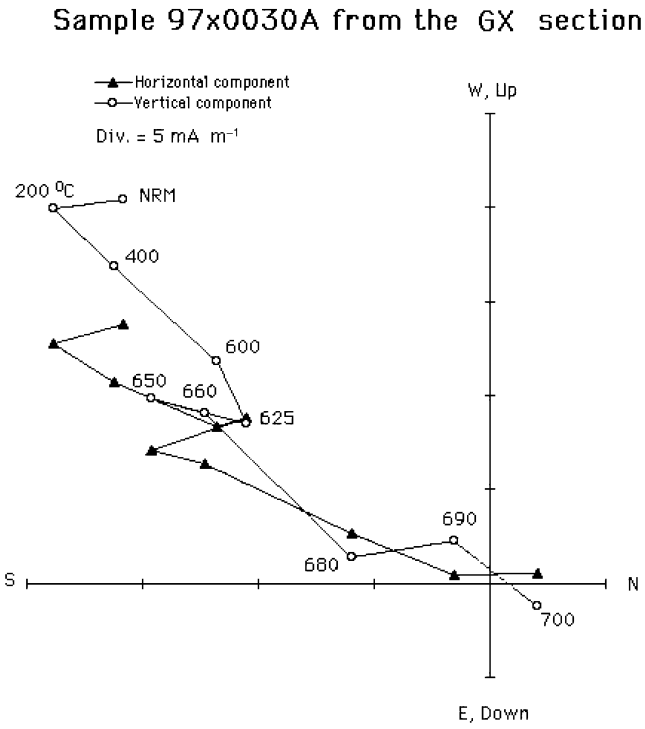

Figure 7. (*Continued.*)

The very high unblocking temperature component (HTC) was isolated between 600 and 690 °C in 82 samples (Table 2). The ChRM directions associated with this HTC were mainly determined by best-fitting lines to vector plots of demagnetization data, but for some samples with overlapping LTC and HTC, a remagnetization circle technique was used. High unblocking temperatures (∼680 °C) and the red pigments of the rocks suggest the magnetic carrier was haematite in each case. The lower part of section GS mainly consists of reversed polarity, whereas the upper part has normal polarity. The normal and reversed polarity magnetic components form polarity zones, which allow us to construct a polarity column (Fig. 8c). However, the two polarities are not exactly antipodal (Table 2), probably due to the overprints by the recent field that are spread throughout the measured section. Although the mean direction for normal-polarity samples (33) fails a fold test, the reversed samples (49 out of a total of 82) pass the fold test at more than 99 per cent confidence (Table 2). The overall site-mean direction is quite consistent with other sections, with an average $D = 20.8^\circ$, $I = 41.8^\circ$ with $k = 4.1$ and $a_{95} = 8.8^\circ$ in stratigraphic coordinates.

4.5 Sections GX and YP

In the Erdaogou area, we collected a total of 239 samples from section GX and 47 samples from section YP, which is continuous with section GX. Progressive thermal demagnetization revealed two components of magnetization, consistent with the observations discussed above. The demagnetization results are rather straightforward: the high stability showed by the normally magnetized sample 98X7008 from the YP section (Fig. 7d) and the reversed polarity sample 97X0030A from the GX section (Fig. 7e) is common in a high proportion of the samples from these two sections. The data corresponding to the HTC display both polarities, but the results of a reversal test are not conclusive (Table 2). Figs 8(d) and (e) illustrate the normal and reversed polarity zones at the GX and YP sections. The fold test results on the HTC, however, are positive at the 99 per cent confidence level in all cases (see Table 2), suggesting that the ChRM was acquired before the folding during the Early Miocene. The global average of ChRM directions for these two sections in stratigraphic coordinates is $D = 13.1^\circ$, $I = 39.0^\circ$, $N = 94$ sites, with $k = 8.0$ and $a_{95} = 5.5^\circ$ (Table 2).

5 REMANENCE DIRECTIONS AND POLARITY SEQUENCES

In summary, palaeomagnetic results from rock samples for this study in the Hoh Xil Basin were magnetically straightforward with two distinct magnetization components: (1) an intermediate unblocking-temperature component, resembling the geocentric axial dipole field direction at the sampling localities and (2) a higher unblocking-temperature component, well defined in vector plots, the remanence of which resides in haematite. Both normal and reversed polarities of the characteristic directions were observed from the stratigraphic sequences of the six measured sections (Table 2). The directions for sections GG1 and GG2 in the Wudaoliang area are generally directed to the northeast, whereas those of the Fenghuoshan sections are northerly (Fig. 9), indicating some clockwise deflection of the directions between these strata. Thus, our data suggest that rocks of the Wudaoliang area may have undergone clockwise rotation. We will return to these results in the next section after a brief discussion concerning the age of magnetization and magnetostratigraphic interpretation.

5.1 Age of magnetization

The directions associated with the ChRM in the red sandstones of the Fenghuoshan and Yaxicuo Groups displayed high consistency with both normal and reversed polarities and were isolated after the present-day field overprinting component (ITC) was successfully removed. Although presented only by a small percentage of samples, the ITC component with reversed polarity would suggest that the ChRM was acquired at least before 0.78 Ma. The fact that almost the same magnetization direction and the same polarity pattern were observed from contemporaneous sites, such as GG1 and GG2, gives us confidence in our results. The fold test results on the ChRM are positive, leading us to interpret the ChRM as being primary (Table 3). In addition, the same ChRM directions have been reported by previously studies (e.g. Halim *et al.* 1998) from the same formation in the same general area (see Table 2), suggesting a primary magnetization has been retained.

Assuming the above are correctly estimated, several critical questions still remain: could the ChRM represents a regional prefolding remagnetization? Regional remagnetizations would probably be related to the India–Asia collision. Regardless of when this remagnetization could have taken place in pre-Early Miocene time (age of folding), the discrepancy between paleolatitude predicted by the APWP and that of Hoh Xil implies at least 12°–24° (∼1200–2400 km) of northward shortening (see the further discussion in Section 6.2). There is no evidence of such a large motion between Tibet and Siberia in such recent times. This information, taken together with the presence of both polarities in the stratigraphic sequences, argues strongly against the hypothesis of a regional remagnetization. Our preferred interpretation is that the magnetizations determined in the present study were records of the palaeomagnetic field close in age to the deposition of these red sandstones.

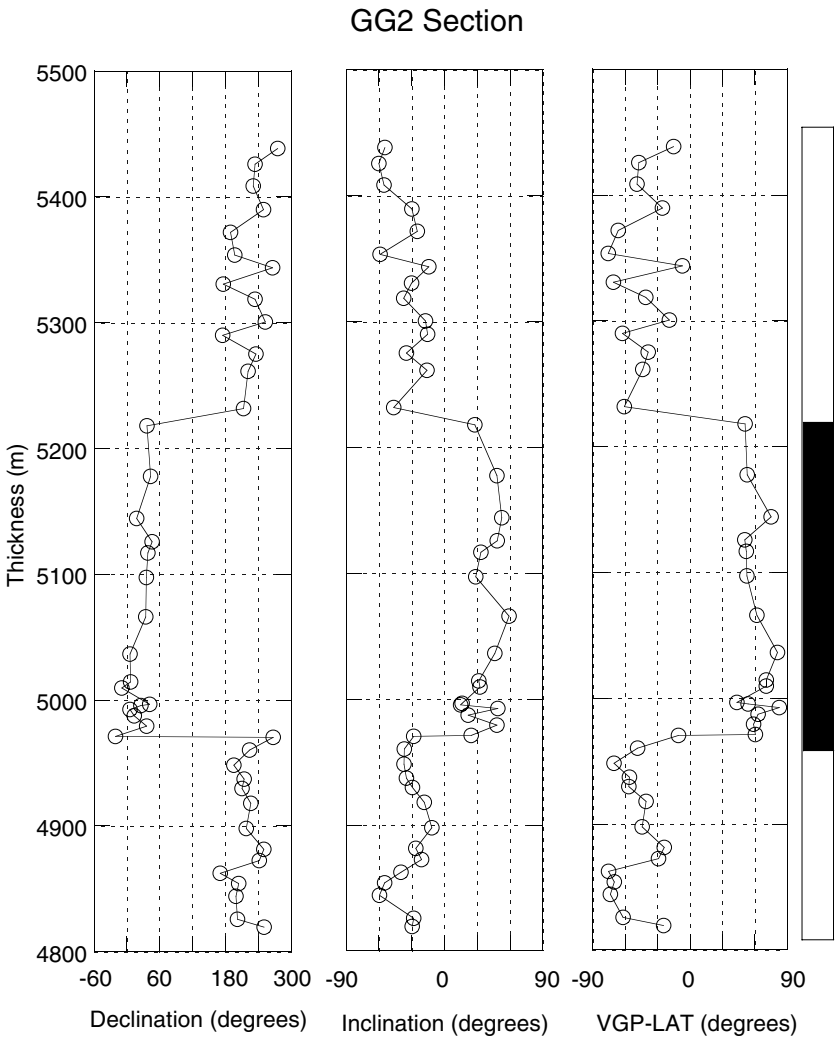

Figure 8. Variations of declination, inclination and virtual geomagnetic pole (VGP) latitude for (a) GG2 section; (b) SP section; (c) GS section; (d) YP section; and (e) GX section. Proposed polarity zones for each section are also shown.

5.2 Polarity column and magnetostratigraphic interpretation

Based on our recognition of reversed and normal polarity ChRM components at the six measured sections, a number of clearly defined magnetic reversals can be discerned from these sections. We can construct a magnetostratigraphic column for the composite section in the Hoh Xil Basin, which features 13 magnetozones (Fig. 10). Each of the major polarity zones is defined by several samples of the same polarity. As with most applications of magnetostratigraphy, one of the greatest problems is the correct matching of the observed sequence of magnetic polarity zones with the appropriate part of the GPTS. For the Hoh Xil Basin, because the observed polarity sequence is defined from the sedimentary succession that is more or less continuous through time, this matching would be straightforward if available biostratigraphic data can assist in deciding which observed magnetic polarity zone or set of zones should be correlated with which magnetic chron on the GPTS. Fortunately, in this combined study several new fossils were collected from the lower part of section YP and the upper part of section GG2, respectively. Biostratigraphic samples between a depth interval of 5438.5 and 4782.8 m have yielded Ostracoda and Gasteropod fossils such as *Artemisia*, *Chenopodiaceae*, *Gramineae*, *Cperaceae*, *Umbelliferae*, *Alnus*, *Eucypris qaibeigouensis* (Sun), *Eucypris lenghuensis* (F. Yang), *Candoniella albicans* (C. Brady), *Suzini* (Schenider), *Cyprinotus* sp., *Obtusochara brevicylindrica* (Xu & Huang), *Tectocharahoui* (S. Wang), *Amblyochara subeiensis* (Huang & Xu), *Hornichara qinghaiensis* (Di), *Obtusochara sp*. *Pterisisporites*, *Classopollis*, *Podocarpidites*, *Pinacae*, *Ephedripites*, *Meliaceoipites* and *Tricolporopollenites.* These fossil assemblages have been assigned ages in the latest part of the Early Oligocene (Liu 1999). Thus, the observed predominantly positive inclinations in this interval suggest that these sediments were deposited within chrons C11 and C12 (30.1–31.3 Ma). This match should be the case because the normal polarity zone is the only normal subchron of this particular age. Similarly, fossils found from a bio-limestone bed (20 cm thick) in the lower part of section YP included Chareae: *Rhabdochara*? sp., *Peckichara subsphaerica*? (Lin & Wang), Cyrogoneae gen, indet., Ostracoda: *Cypris* sp., Gasteropod: *Sinoplanorbis* sp., *Amnicola* sp., *Bithynis* sp., *Cyathidites* sp., *Schizosporites* sp., *Pediastrum* sp. They have been assigned ages ranging from the Middle and the Late Eocene (Yi *et al.* 1990). Therefore, the shift in polarity from reverse to normal at a depth of 1979.2 m within the YP section would correspond to the onset normal subchron in chron C18.

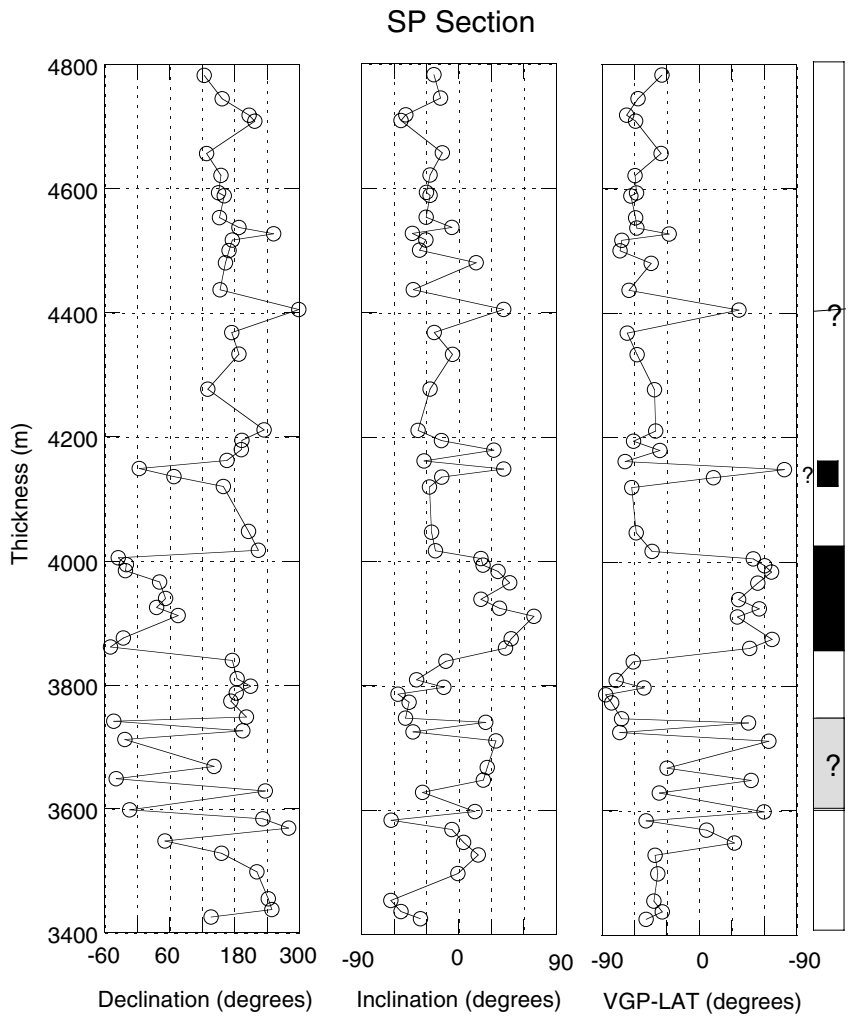

Figure 8. (*Continued.*)

We have used these age constraints and spacings of the observed polarity intervals to anchor our polarity column to the geomagnetic timescale (Cande & Kent 1995) (Fig. 10). Several first-order conclusions can be drawn from these correlations. Our new magnetostratigraphic correlation indicates that sediments in the Fenghuoshan Group were deposited approximately 51–31 Myr (Early Eocene–Early Oligocene), and the age of the Yaxicuo Group is between 31 and 30 Ma (Early Oligocene). The sediments in the Hoh Xil Basin, therefore, are definitely not Cretaceous in age. This inference is strongly supported by the facts that the present study is the first place of the Hoh Xil Basin where dense sampling through the sediments has been carried out and yet there is no indication in the magnetic record for the long normal polarity zone (chron C34, between 118 and 83 Ma) in the Cretaceous (Cande & Kent 1995).

5.3 Sedimentation rates

The Tertiary sediments of the Hoh Xil Basin composite section have yielded a detailed magnetic polarity stratigraphy (Fig. 10), from which relatively precise sedimentation rates can be calculated. Because nearly all intervals are represented by multiple samples, it would appear that the continuity of sedimentation and sampling density at each site was adequate to record and identify each polarity interval, albeit minimally in a few places. As shown in Fig. 11, the sediment-accumulation rates at the Hoh Xil Basin exhibit alternating high and low values, with four periods (43.8–42.5, 40.1–39.5, 38.4–34.7 and 33.6–30.1 Ma, respectively) and that the averaged rates exceed 200 m Myr^{-1}. These relative high sedimentation rates are consistent with the strongest denudation and uplift rates deduced from geological observations for the same time intervals (Liu & Wang 1999, 2001; Wang *et al.* 1999), suggesting that they were probably caused by intracontinental convergence between India and Eurasia and better constraints of the timing of deformation can be obtained. Sedimentation rates reached ∼1529 m Myr^{-1} during the Middle Eocene (∼40 Ma), much higher than the averaged rate of 200 m Myr^{-1}, both before and after this time interval (Fig. 11). Interestingly, there is an apparent coincidence in time between this high sedimentation rate and known aspects of tectonic evolution of the region. The northward drifting rate of India also decreased dramatically at this time, from ∼1000 m Myr^{-1} between 70 and 40 Ma to ∼500 m Myr^{-1} at 40 Ma (Molnar & Tapponnier 1975). If uplifting results in mountains growing faster than rivers can incise them, the interior of the basin could become flooded with sediments eroded from the surrounding mountains (Tapponnier *et al.* 2001). However, we are also well aware that

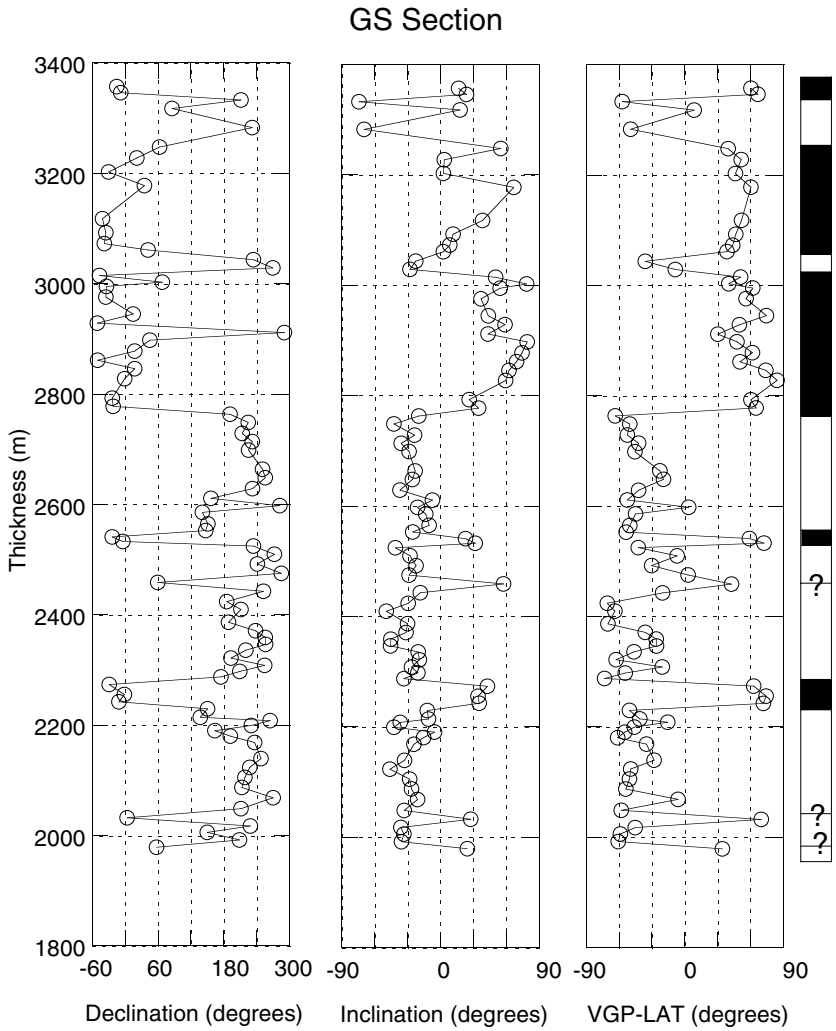

Figure 8. (*Continued.*)

occasionally high sedimentation rates could be caused by hiatuses. Indeed, several short hiatuses (or decreases in accumulation rates) are inferred within the Fenghuoshan Group (Fig. 11). The sedimentation rate is an estimate based on the datum directly above and below the interval. Thus the sedimentation rate should be seen as an approximation because there are few dates to use for the reliable determination.

More detailed work and improved methods are needed to better detect this apparently high sedimentation rate.

6 TECTONIC ANALYSIS AND DISCUSSION

6.1 Clockwise rotation of the Wudaoliang area

In Table 4, the Tertiary palaeomagnetic results from the Hoh Xil Basin (Table 2) are compared with coeval reference poles for Eurasia (30–60 Ma poles of Besse & Courtillot 1991) were transferred from North America, Africa and India using ocean kinematics. As mentioned, previous palaeomagnetic studies (with adequate magnetic cleaning techniques) on sedimentary rocks of the Hoh Xil Basin include Lin & Watts (1988) and Halim *et al.* (1998). These palaeomagnetic data come from a single sampling locality in the Fenghuoshan area and the directions agree with ours very well. We have re-analysed their data in terms of a combined fold test (Tables 2 and 4). It is obvious from the data in Table 4 that sections in the Fenghuoshan area show no relative rotations as demonstrated by the fact that the observed declinations are not significantly different from those expected to be inferred from the contemporaneous Eurasian poles (Table 4 and Fig. 8). On the other hand, the mean palaeomagnetic declinations for the GG sections are deflected clockwise from the expected directions for Eurasia. A clockwise vertical-axis block rotation of $29.1^\circ \pm 8.5^\circ$ of the sampling area since the Oligocene is implied by the data (Table 4 and Fig. 9). Palaeocurrent and provenance indicators for the Yaxicuo Group (Liu 1999) as well as the overturning of strata in the GG1 section are all testimony to the fact that intraplate deformation is stronger in the Wudaoliang area compared with those in the Fenghuoshan area. Although our palaeomagnetic investigation is not sufficiently detailed to consider the problem of rotation mechanism and the timing of the rotation, we note that there is a major NW–SE-trending fault near the sampling area (Fig. 4), which may be responsible for causing the rotation by its simple shear deformation.

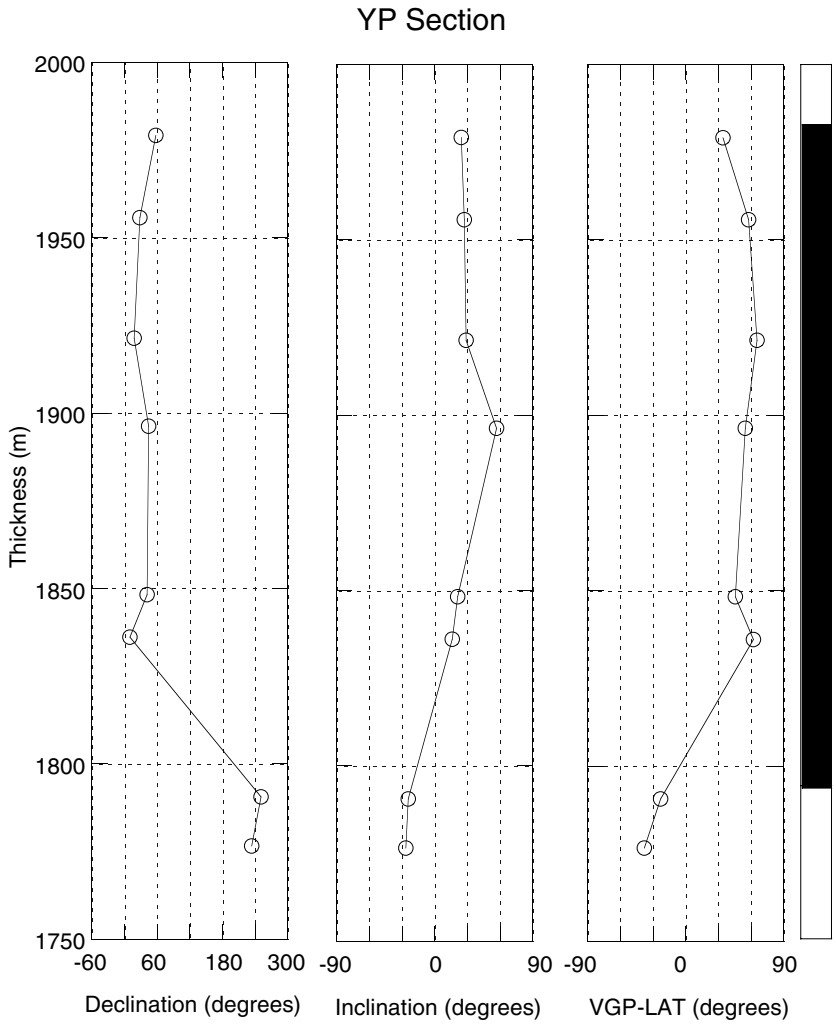

Figure 8. (*Continued.*)

6.2 The Tertiary low-paleolatitude dilemma in central Asia

Palaeomagnetic data in Table 4 clearly show that the Hol Xil Basin did not occupy its current position in terms of paleolatitude in the Tertiary. The mean palaeolatitudes predicted for the Hol Xil Basin is 21° within a 95 per cent confidence band of only ±4°. The palaeomagnetically inferred latitudinal displacements (*F* values in Table 4) are statistically significant and the positive (northward) magnitudes are significantly different from zero. Our results agree with the consistent pattern of disturbingly low palaeolatitudes derived from a large number of high-quality palaeomagnetic studies. From Kyrgyzstan and the western Tianshan all the way to eastern China, the inclinations of stable magnetization are anomalously shallow (Achache *et al.* 1984; Otofuji *et al.* 1989, 1991; Chen *et al.* 1991; Meng 1991; Pozzi & Feinberg 1991; Huang & Opdyke 1992; Gilder *et al.* 1996, 1999, 2001; Thomas *et al.* 1993, 1994; Zhao *et al.* 1994, 1996; Cogne *et al.* 1995; Chauvin *et al.* 1996; Halim *et al.* 1998; Cogne *et al.* 1999; Rumelhart *et al.* 1999). Using the 40 and 60 Ma Eurasian reference poles of Besse & Courtillot (1991), Cogné *et al.* (1999) showed that the inclinations translate to palaeolatitudes 5°–25° lower than expected—that is, ranging from an average of 8°–12° in the east to 15°–21° further west. The northward displacements relative to Siberia implied by these low palaeolatitudes are larger by several times or more than estimates of shortening from crustal thickening in intervening mountain belts.

It is important to understand the meaning of the discordance between the palaeomagnetic poles for central Asia and Eurasia. Inclination error, the spurious shallowing of inclination of sedimentary magnetization that occurs during deposition and especially compaction of some sedimentary rocks, is one obvious candidate (Anson & Kodama 1987; Arason & Levi 1990a,b; Deamer & Kodama 1990). It has been implicated as a major cause of anomalously low palaeomagnetic palaeolatitudes inferred from turbidites of the North American Salinian and Peninsular terranes: compaction and remanence-anisotropy experiments on these rocks indicate 10°–17° of shallowing relative to the inclination of the magnetizing field (Kodama & Davi 1995; Dickinson & Butler 1998; Tan & Kodama 1998). In the case of central Asia the low palaeolatitudes are recorded predominantly in red beds, and in most cases haematite is the main carrier of remanence. Therefore, it could be chemical in origin and not subject to inclination error. Indeed, inclinations of red beds from the above-mentioned Salinian terrane are not anomalously shallow, nor are those from Cretaceous red beds of the North China Block and the Tadjik depression (Pozzi & Feinberg 1991; Bazhenov *et al.* 1994; Zhao *et al.* 1996). Moreover, in some cases a succession of red beds with large variations in grain size and

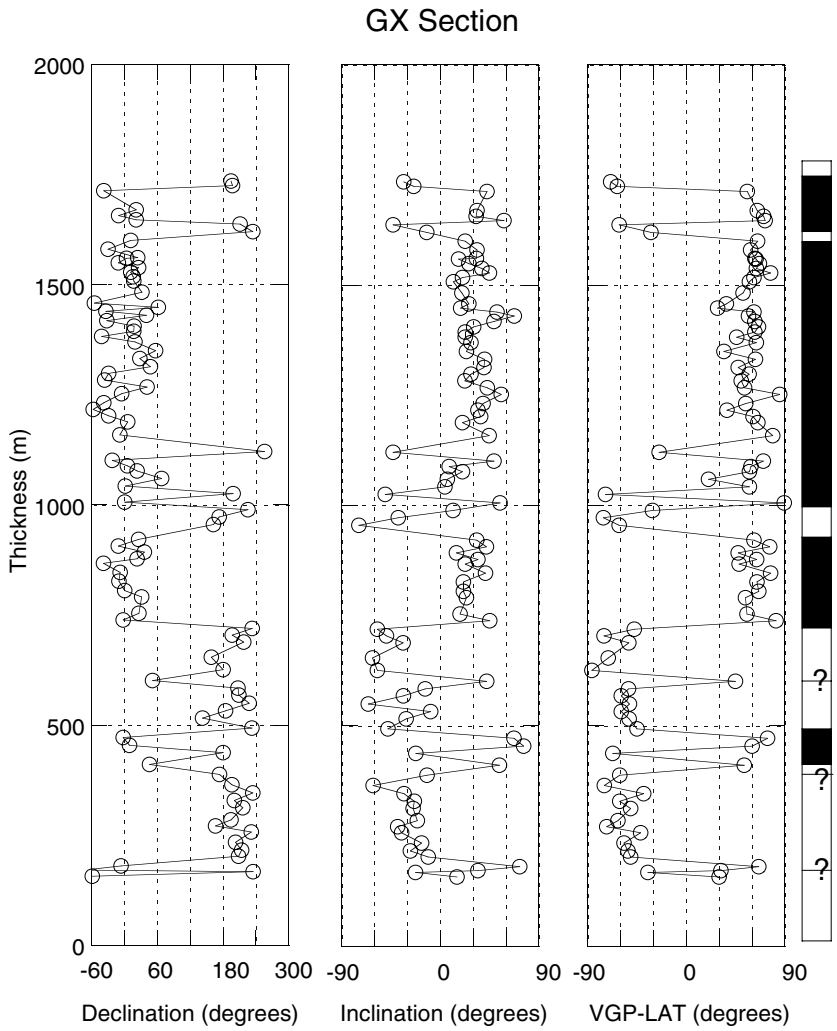

Figure 8. (*Continued.*)

percentage of clay all exhibit the same inclination (Thomas *et al.* 1994), contrary to expectations for compaction shallowing (Tan & Kodama 1998). Several arguments also exist against post-depositional compaction shallowing (Gilder *et al.* 2001). On the other hand, a substantial inclination error has been demonstrated in modern red deposits (Tauxe & Kent 1984) and has been suggested on the basis of compaction experiments on redeposited red bed sediment from one formation in northwest China (Tan et al. 1996). Considering all of this information together, it seems likely that the inclination error might be a significant source of shallowing in some, but not all of the anomalous Tertiary results.

If there were a huge systematic error in the ages, so that instead of Tertiary the rocks were really Cretaceous, this would solve much of the problem. Then the larger paleolatitude anomalies would be reduced and no large-scale extension would be necessary. It is true that the ages of continental red sandstones are notoriously difficult to pin down accurately. Fossils are rare and usually not as diagnostic as required, and tying these formations into regional stratigraphic columns often involves lateral facies correlations, which can be quite subjective. However, although many of the Tertiary ages assigned to the various palaeomagnetic results can be legitimately questioned, it is unlikely that their real ages are all much older. Therefore, while an extreme paleolatitude anomaly of a particular Tertiary result would be cut in half by instead assuming its age to be Cretaceous, this is not a general solution to the low-paleolatitude problem.

The only other plausible explanation is that the Eurasian reference poles are not appropriate for Siberia. Since none of them come from rocks in Siberia, this is a real possibility. In fact, the only data from Eurasia with ages between 35 and 70 Ma of high enough quality to be used for a reference pole are those from the British Tertiary Igneous Province, some 4000 km to the west (Van der Voo 1993). Consequently, the synthetic reference APW path for Eurasia during this time consists almost entirely of poles transferred from North America (nine poles), Africa (three) and India (one) (Besse & Courtillot 1991). However, Bazhenov & Mikolaichuk (2002) recently reported a palaeomagnetic pole from mid-Late Palaeocene basalt in Kirgyzstan that coincides with the Eurasian pole as derived from the North Atlantic Igneous Province. Although better defined data are still needed, anomalous inclinations from central Asia are unlikely due to errors introduced by transferring poles to Eurasia.

Another potentially significant source of error, however, is the non-rigid behaviour of Eurasia. For example, Cogné *et al.* (1999)

Table 2. Summary of characteristic palaeomagnetic results from the Hoh Xil Basin.

Section ID	*R*/*N*	Range (°C)	G_Dec	G_Inc	S_Dec	S_Inc	S_Long	S_lat	a_{95}	k2
This study										
Wudaoliang area (93.00°E, 34.98°N), red and grey sandstone of Yaxicuo Group										
GG1	3/12	600–685	97.3	−34.4	52.7	55.3	165.9	47.6	12.9	9.7
GG2	28/16	600–700	61.4	32.1	33.5	35.5	201.6	56.7	7.3	9.8
GG1+GG2	31/28	600–700	69.5	18.6	37.2	40.8	188.8	57.4	10.5	54.1
Normal	0/28		72.8	10.7	31.7	45.8	190.2	61.9	9.7	8.9
Reversed	31/0		247.1	−23.9	221.6	−36.0	14.2	−50.5	9.2	8.8
Sangqiashan area (92.98°E, 34.60°N), purple siltstone and sandstone of Fenghuoshan Group										
SP	36/15	550–700	296.5	59.4	357	37.4	284.7	76	8.3	6.8
Normal	0/15		288.2	48.9	346.9	37.2	316.2	72	15.8	6.8
Reversed	36/0		121.4	−63.4	181.2	−37.3	88.3	−76.2	9.8	6.9
GS	49/33	600–690	359.5	73.2	20.8	41.8	207.5	69.1	8.8	4.1
Normal	0/33		348.3	53.5	354	45	307.2	80.5	11.6	5.6
Reversed	49/0		234.3	−84.2	217.4	−36.1	16.8	−54	11.2	4.3
Erdaogou area (92.74°E, 34.56°N), purple siltstone and sandstone of Fenghuoshan Group										
YP	2/5	625–685	72.8	53.9	37.1	29.8	202.5	52	17.7	12.6
Normal	0/5		61.8	59.7	26.5	30.1	213.8	60	19.5	16.3
Reversed	2/0		270.6	−36.7	242.2	−25.7	7	−30.4		51.1
GX	32/55	625–700	290.3	85.2	10.8	39.6	231.9	74.7	5.7	8
Normal	0/55		292	79.1	3.4	40	257.7	77.8	7.2	8.1
Reversed	32/0		295.9	−84.5	203	−38	29.9	−65.9	8.8	9.2
YP+GX	34/60	625–700	326.5	87.1	13.1	39	226.6	73.1	5.5	8
Normal	0/60		306.1	81.4	5.7	39.3	249.1	76.7	6.8	8.2
Reversed	34/0		286.6	−81.8	205.7	−37.6	26.8	−63.7	8.8	8.9
Overall Mean for Fenghuoshan Group: $N = 4$ sections (SP, GS, YP and GX)										
(k2/k1 = 3.1)			2.1	78.5	16.7	37.8	221	70.4	17	30.3
Mean $N = 3$ (SP, GS and YP+GX)										
(k2/k1 = 2.9)			320	75	9.9	39.5	233.7	75	17.8	61.8
Previous study, Fenghuoshan area (92.7°E, 34.5°N)										
Halim *et al.* (1998) $N = 7$			306.3	48.5	9.5	34.3	242	72.2	8.9	47
Lin & Watts (1988) $N = 12$ sites					215	−34	21	−55.0	4.9	79
Average with Halim *et al.* (1998)										
$N = 5$ sections (k2/k1 = 4.4)			335.9	74.2	15.2	38.2	224.9	71	12.5	38.2

Explanation: range—range of unblocking temperatures of component during thermal demagnetization. R/N, number of reversed (R) to number of normal (N) samples. G_Dec/G_Inc, S_Dec/S_Inc, declination and inclination in geographic and stratigraphic coordinates, respectively; S_Long/S_Lat, east longitude and north latitude of VGP in stratigraphic coordinates; a_{95}/A_{95}, radius of the circle of 95 per cent confidence concerning the direction/VGP in degrees (stratigraphic coordinates). k2(k1)/K, Fisher (1953) precision parameter for direction after (before) tilt correction/for VGP.

Table 3. Fold and reversal test results on ChRM.

Section ID	(°E, °N)	*R*/*N*	SCOS *in situ*	SCOS Tilt-corrected	SCOS *95 per cent	SCOS **99 per cent	r_o (deg)	r_c (deg)
GG1 (all)	93.00°E, 34.98°N	3/12	4.244	2.250	4.510	6.305	13.1	32.3
GG2 (all)	93.00°E, 34.98°N	28/16	4.930	0.855	7.716	10.910	12.9	14.7
GG1+GG2 (normal)	93.00°E, 34.98°N	0/28	23.793	0.629	6.155	8.703		
GG1+GG2 (reversed)	93.00°E, 34.98°N	31/0	7.142	4.750	6.476	9.157		
GG1+GG2 (all)	93.00°E, 34.98°N	31/28	35.513	1.737	8.935	12.633	12.2	13.2
SP (normal)	92.98°E, 34.60°N	0/15	4.728	1.536	4.510	6.305		
SP (reversed)	92.98°E, 34.60°N	36/0	8.233	3.717	6.979	9.868		
SP (all)	92.98°E, 34.60°N	36/15	11.436	4.065	8.307	11.746	12.9	18.1
GS (normal)	92.98°E, 34.60°N	0/33	16.106	10.531	6.682	9.448		
GS (reversed)	92.98°E, 34.60°N	49/0	17.279	2.392	8.142	11.513		
GS (all)	92.98°E, 34.60°N	49/33	30.917	6.748	10.533	14.894	30.4	15.9
SP+GS (all)	92.98°E, 34.60°N	85/48	34.058	0.308	13.415	18.968	22.5	11.4
YP (all)	92.74°E, 34.56°N	2/5	0.049	1.432	3.086	4.253	31.6	32.7
GX (normal)	92.74°E, 34.56°N	0/55	14.395	2.451	8.626	12.198		
GX (reversed)	92.74°E, 34.56°N	32/0	9.781	0.557	6.580	9.304		
GX (all)	92.74°E, 34.56°N	32/55	24.491	0.704	10.850	15.341	15.3	11.5
YP + GX (normal)	92.74°E, 34.56°N	0/60	18.964	1.016	9.010	12.740		
YP + GX (reversed)	92.74°E, 34.56°N	34/0	11.524	1.562	6.783	9.590		
YP + GX (all)	92.74°E, 34.56°N	34/60	31.805	3.066	11.278	15.946	15.6	11.1

Note: R/N = number of reversed (R) to number of normal (N) samples; r_o = angle between normal and reversal mean directions; r_c = critical angle of McFadden & McElhinny (1990). *, **: 95 and 99 per cent critical SCOS values for the structural correction using definition 2 of SCOS in the test of McFadden (1990), which must be exceeded for significant correlation.

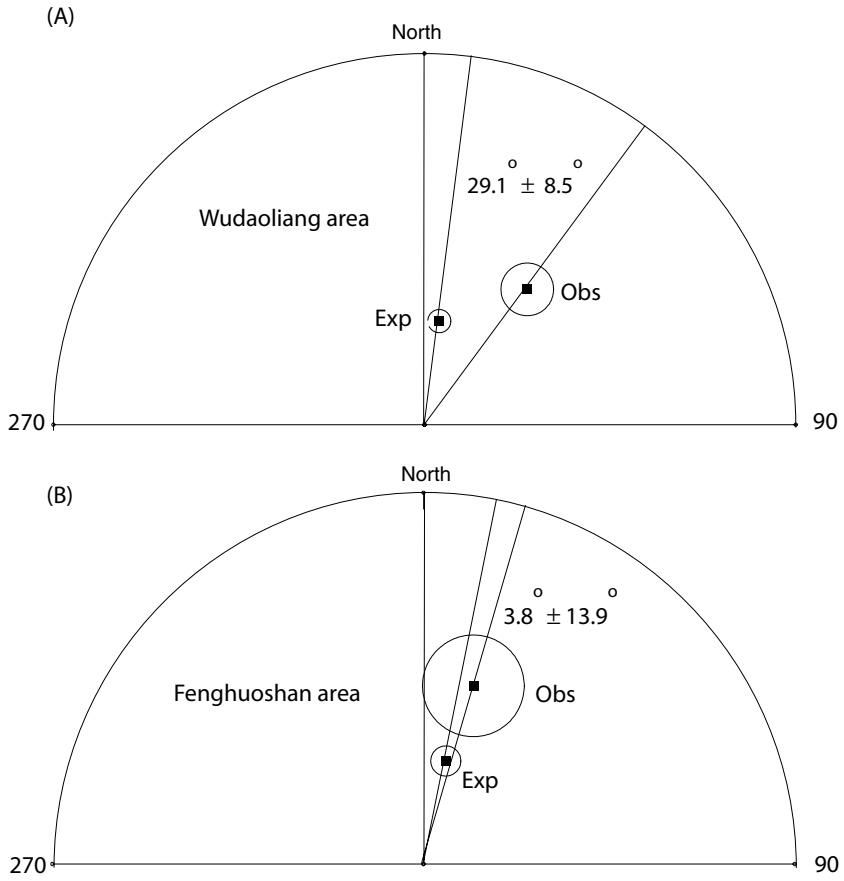

Figure 9. Equal-area projection of magnetic directions with 95 per cent confidence circles for the two areas in Hoh Xil basin listed in Table 4. (a) Wudaoliang area, (b) Fenghuoshan area. Obs = observed; Exp = expected directions reduced from the Eurasian poles.

have pointed out that fairly small amounts of compression or extension in western Europe could produce much larger southward relative movements in Asia because of the large lever-arm effect. The fairly good agreement of Late Permian and Early Triassic poles from Europe and Siberia suggest that this mechanism could not account for more than approximately half of the paleolatitude anomaly (Smethurst *et al.* 1998). Our own Tertiary and Late Cretaceous palaeomagnetic data from Siberia also do not support the hypothetical non-rigid behaviour (Zhao *et al.* 2001, 2002).

7 CONCLUSIONS

The polarity patterns from the red sedimentary sequence of the Fenghuoshan and Yaxicuo Groups at the Hoh Xil Basin show that a reliable magnetostratigraphy can be established for the past 52 Ma. The magnetostratigraphic profile features 13 polarity chrons and correlates well with chrons C23–C11. The age of the Fenghuoshan Group is palaeomagnetically dated as 51–31 Ma (Early Eocene–Middle Early Oligocene), and the age of the Yaxicuo Group is between 31 and 30 Ma (Middle Early Oligocene–Late Early Oligocene). The new palaeomagnetic data from the Fenghuoshan Group suggest that it has undergone no significant rotation since the Oligocene. In contrast, declination data from the Yaxicuo Group in the Wudaoliang area imply a vertical-axis clockwise rotation (29.1° ± 8.5°) since the Late Oligocene.

The Tertiary palaeomagnetic pole position of the Hoh Xil Basin implies a significant northward convergence with respect to Eurasia (Siberia) since Early Eocene–Late Oligocene times. The differences between the observed palaeolatitudes from this study and those expected from palaeomagnetic reference poles for Eurasia are much larger than geological estimates of crustal shortening. Our results are consistent with the pattern of disturbingly low palaeolatitudes derived from a large number of high-quality palaeomagnetic studies of Tertiary rocks in central Asia. More rock-magnetic and palaeomagnetic data are needed to separate the influences of rock-magnetic characteristics, sedimentary inclination shallowing and tectonic shortening.

ACKNOWLEDGMENTS

Discussions with our many colleagues have been most stimulating and helpful. We thank Xianghui Li, Xiumian Hu, Lidong Zhu, Mingjian Wei, Shifeng Wang and Xiaonan Wang for assistance in the field, and the journal editor and three anonymous reviewers for constructive suggestions on the original manuscript. During various stages of this research, palaeomagnetic software developed by Randy Enkin was often used. XZ wants to extend special thanks to the paleomagnetism group of the Institute for Rock Magnetism at the University of Minnesota for support and fruitful discussions. We are pleased to acknowledge the support of the US National Science Foundation grants EAR-9805444, EAR-9903194 and EAR-0003512, the National Natural Science Foundation of China (40102010) and the National Key Basic Research Science Foundation of China (G1998040800). This manuscript is contribution 424

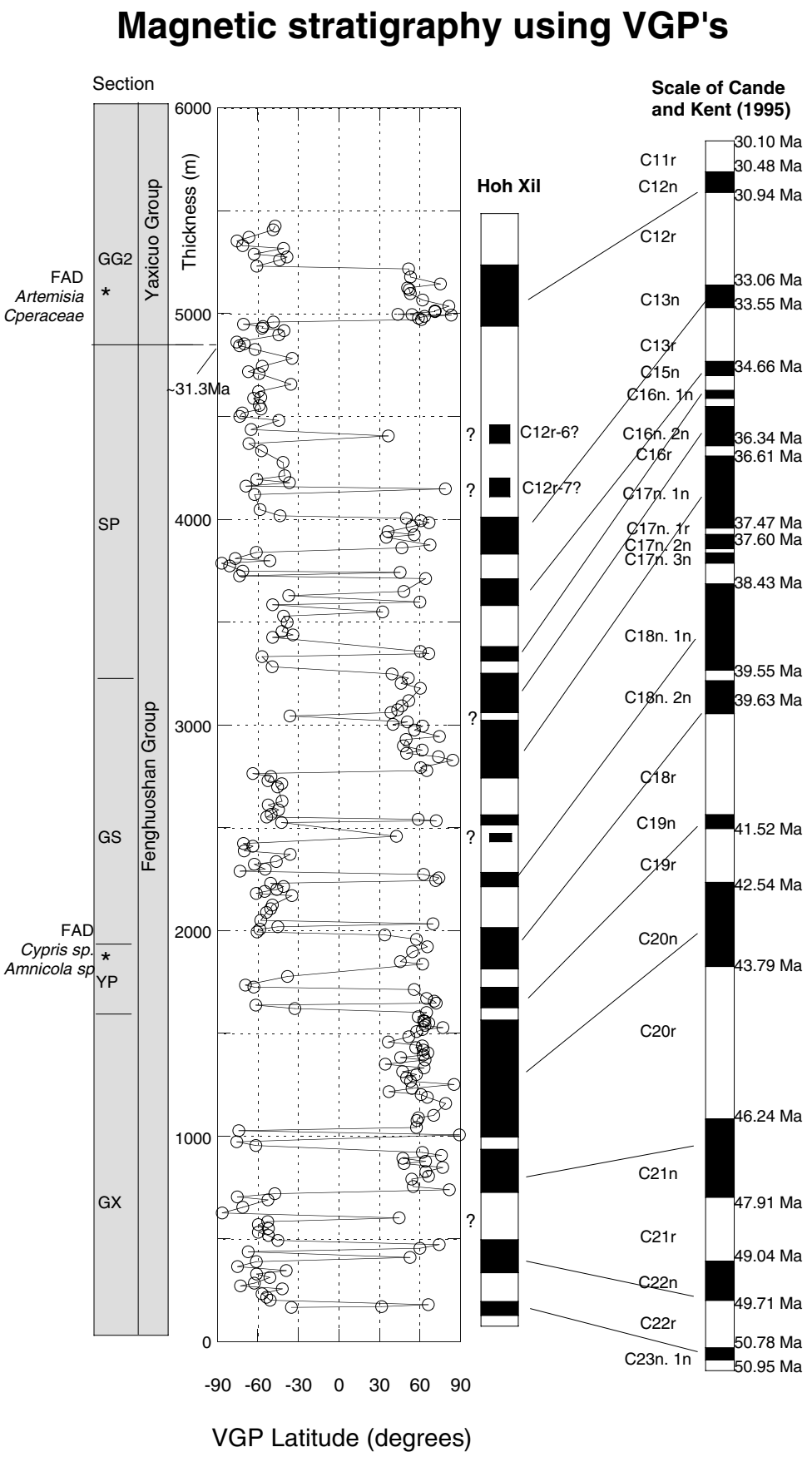

Figure 10. Magnetochronostratigraphy chart of the Hoh Xil basin, northern Tibet and correlation with the reference scale of Cande & Kent (1995). Poorly defined magnetic intervals are indicated by short-half bars and question marks.

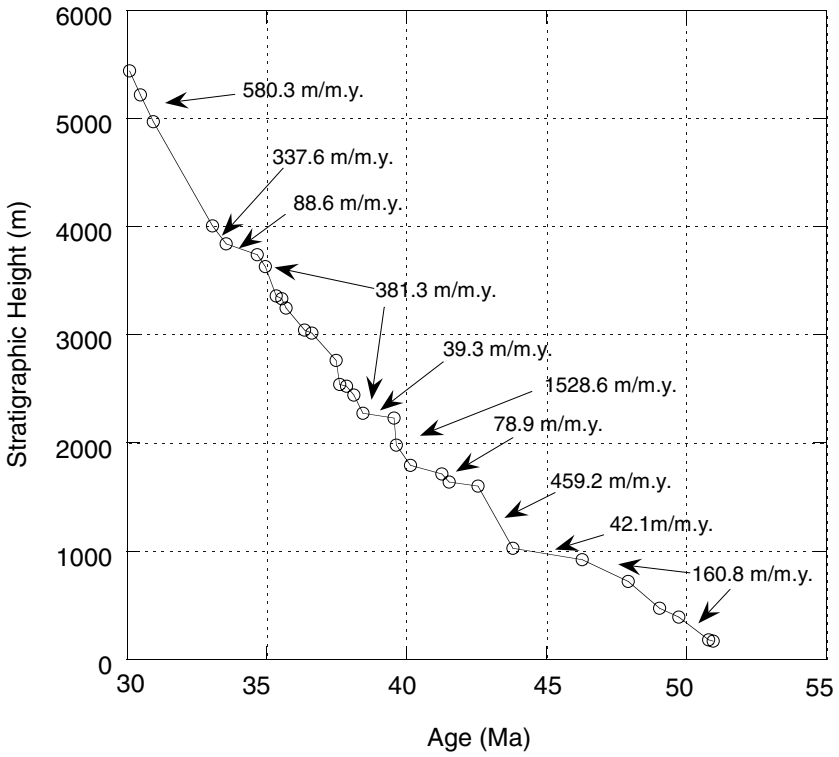

Figure 11. Sediment accumulation rate curve of the Tertiary sediments in the Hoh Xil basin.

of the Center for Studies of Imaging and Dynamics of the Earth, Institute of Geophysics and Planetary Physics and Paleomagnetism Laboratory at the University of California, Santa Cruz.

REFERENCES

Achache, J., Coutillot, V. & Zhou, Y.X., 1984. Paleogeographic and tectonic evolution of south Tibet since Middle Cretaceous time: new paleomagnetic data and synthesis, *J. geophys. Res.,* **89,** 10 311–10 339.

An, Z., Kutzbach, J., Prell, W.L. & Porter, S.C., 2001. Evolution of Asian monsoons and phased uplift of the Himalaya-Tibetan plateau since Late Miocene times, *Nature,* **411,** 62–66.

Anson, G.L. & Kodama, K.P., 1987. Compaction induced shallowing of the post depositional remanent magnetization in a synthetic sediment, *Geophys. J. R. astr. Soc.,***88,** 673–692.

Arason, P. & Levi, S., 1990a. Compaction and inclination shallowing in deep sea sediments from the Pacific Ocean, *J. geophys. Res.,* **95,** 4501–4510.

Arason, P. & Levi, S., 1990b. Models of inclination shallowing during sediment compaction, *J. geophys. Res.,* **95,** 4481–4510.

Argand, E., 1924. La tectonique de l'Asie, in *Proc. 13th Int. Gélogues Congrès,* Vol. 7, pp. 171–372, Brussels.

Bazhenov, M.L. & Mikolaichuk, A.V., 2002. Paleomagnetism of Tertiary basalts from the Tien Shan, Kirgyzstan: rigid Eurasia and the dipole geomagnetic field, *Earth planet. Sci. Lett.,* **195,** 155–166.

Bazhenov, M.L., Perroud, H., Chauvin, A., Burtman, V.S. & Thomas, J.C., 1994. Paleomagnetism of Cretaceous red beds from Tadzhikistan and Cenozoic deformation due to India–Eurasia collision, *Earth planet. Sci. Lett.,* **124,** 1–18.

Beck, M.E. & Schermer, E.R., 1994. Aegean paleomagnetic inclination anomalies: is there a tectonic explanation?, *Tectonophysics,* **231,** 281–292.

Beck, R.A., Burbank, D.W., Sercombe, W.J., Khan, A.M. & Lawrence, D., 1996. Late Cretaceous ophiolite obduction and Paleocene India–Asia collision in the westernmost Himalaya, *Geodinamica Acta,* **9,** 114–144.

Berggren, W.A., Kent, D.V., Swisher, C.C., III & Aubry, M.-P., 1995. A revised Cenozoic geochronology and chronostratigraphy, in *Geochronology, Time Scales and Global Stratigraphic Correlation,* pp. 129–212, eds Berggren, W.A., Kent, D.V., Aubry, M.-P. & Hardenbol, J., Spec. Publ. SEPM, 54.

Besse, J. & Courtillot, V., 1991. Revised and synthetic apparent plar wander paths of the African, Eurasian, North American and Indian plates, and true polar wander since 200 Ma, *J. geophys. Res.,* **96,** 4029–4050.

BGMRQ (Bureau of Geology and Mineral Resources of Qinghai), 1991. Regional geology of Qinghai, pp. 1–662, Geological Publishing House, Beijing (in Chinese with English abstract).

Cande, S.C. & Kent, D.V., 1992. A new geomagnetic polarity time scale for the Late Cretaceous and Cenozoic, *J. geophys. Res.,* **97,** 13 917–13 951.

Cande, S.C. & Kent, D.V., 1995. Revised calibration of the geomagnetic polarity time-scale for the Late Cretaceous and Cenozoic, *J. geophys. Res.,* **100,** 6093–6095.

Channell, J.E.T., Erba, E., Nakanishi, M. & Tamaki, K., 1995. Late Jurassic–Early Cretaceous time scales and oceanic magnetic anomaly block models, in *Geochronology, Time Scales and Global Stratigraphic Correlations,* pp. 51–63, eds Berggren, W.A., Kent, D.V., Aubry, M.-P& Hardenbol, Spec. Publ. SEPM, 54.

Chauvin, A., Perroud, H. & Bazhenov, M.L., 1996. Anomalous low paleomagnetic inclinations from Oligocene–Lower Miocene red beds of the south-west Tien Shan, Central Asia, *Geophys. J. Int.,* **126,** 303–313.

Chen, Y. *et al.*, 1991. Paleomagnetic study of Mesozoic continental sediments along the northern Tien Shan (China) and heterogeneous strain in central Asia, *J. geophys. Res.,* **96,** 4065–4082.

Chen, Y., Courtillot, V., Cogné, J.P., Besse, J., Yang, Z.Y. & Enkin, R., 1993. The configuration of Asia prior to the collision of India: Cretaceous paleomagnetic contstraints, *J. geophys. Res.,* **98,** 21 927–21 941.

Coe, R.S., Globerman, B.R., Plumley, P.W. & Thrupp, G.A., 1985. Paleomagnetic results from Alaska and their tectonic implications, in *Tectonostratigraphic terranes of the Circum-Pacific region,* pp. 85–108, ed. Howell, D.G., Circum-Pacific Council on Energy and Resources Earth Sciences Series no. 1, American Association of Petroleum Geologists.

Table 4. Tertiary palaeomagnetic poles, palaeolatitudes and tectonic parameters for the Hoh Xil Basin.

Age*	Reference	Pole		Measured		VGP		Observed direction		Expected direction		Tectonic	Parameters	Plat.
(Ma)	Long. (°E)	Lat. (°N)	A95	section	Long. (°E)	Lat. (°N)	A95	$D_o \pm D$	$I_o \pm I_o$	Dex ± Dex	Iex ± Iex	$R \pm R$	$F \pm F$	
20–30	147.6	82.3	3.3	GG	192.7	55.7	6.7	37.2 ± 6.9	40.8 ± 5.2	8.1 ± 4.9	58.5 ± 2.6	29.1 ± 8.5	15.9 ± 5.8	23.3
30	132.8	81	2.7	SP	284.7	76	8.3	357.0 ± 8.2	37.4 ± 6.5	7.7 ± 4.3	60.4 ± 2.1	−10.7 ± 9.2	20.4 ± 6.8	20.9
40	145.4	80.2	3.6	GS	207.5	69.1	8.8	20.8 ± 9.2	41.8 ± 6.9	10.2 ± 5.5	59.3 ± 2.8	10.6 ± 10.7	16.0 ± 7.4	24.1
50	149	77.9	4.3	YP	202.5	52	17.7	37.1 ± 16.0	29.8 ± 13.8	13.3 ± 6.7	59.7 ± 3.4	−22.6 ± 17.3	24.6 ± 14.2	16
60	178.7	78.5	3.9	GX	231.9	74.7	5.7	10.8 ± 5.8	39.6 ± 4.5	14.0 ± 5.2	54.0 ± 3.0	−3.2 ± 7.8	12.1 ± 5.4	22.5
50–60	149	77.9	4.3	YP + GX	226.6	73.1	5.5	13.1 ± 5.5	39.1 ± 4.3	13.3 ± 6.7	59.7 ± 3.4	−0.2 ± 8.7	18.5 ± 5.5	22.1
30–60	152.6	79.8	4.3	FHS	233.7	75	17.8	9.9 ± 18.2	39.5 ± 13.9	11.4 ± 6.4	58.5 ± 3.4	−1.5 ± 19.3	16.7 ± 14.3	22.5
30–60	152.6	79.8	4.3	H+L	210.5	62.6	4	25.5 ± 3.8	34.6 ± 3.1	11.4 ± 6.4	58.5 ± 3.4	14.1 ± 7.4	20.2 ± 4.6	19
30–60	152.6	79.8	4.3	All (N=5)	224.9	71	12.5	15.2 ± 12.3	37.2 ± 9.8	11.4 ± 6.4	58.5 ± 3.4	3.8 ± 13.9	18.4 ± 10.4	20.8

*Eurasia Reference pole by Besse & Courtillot (1991). Lat., Long., latitude and longitude of the north-seeking pole positions, A95, a radius of 95 per cent confidence circle of the pole.
Dec., Inc., declination and inclination reduced at the sampling site, respectively, del-lat, del-d, 95 per cent confidence limit in paleolatitude and declination, respectively, del-lat = C*A95, C = 0.78, del-d = C sin-1 (sin [A95]/cos [Plat.]); Tectonic parameters, *F* and *R*: displacement northward (+) or southward (−) and azimuthal rotation clockwise (+) or counter-clockwise (−) of sampling area with respect to reference blocks, inferred from the difference between the mean palaeomagnetic pole and the coeval reference pole.
del-*F* and del-*R*: uncertainties (95 per cent confidence limits) of F and R, respectively, estimated by the method of Coe *et al.* (1985).
FHS = Fenghuoshan, H+L = Combined results from Halim et al. (1998) and Lin & Watts (1988).

Cogné, J.P., Chen, Y., Courtillot, V., Rocher, F., Wang, G., Bai, M. & You, H., 1995. A paleomagnetic study of Mesozoic sediments from Junggar and Turfan basins, NW China, *Earth planet. Sci. Lett.,* **133,** 353–366.

Cogné, J.P., Halim, N., Chen, Y. & Courtillot, V., 1999. Resolving the problem of shallow magnetizations of Tertiary age in Asia: insights from paleomagnetic data from the Qiangtang, Kunlun, and Qaidam blocks (Tibet, China), and a new hypothesis, *J. geophys. Res.,* **104,** 17 715–17 734.

Coward, W.P., Kidd, W.S.F., Pang, Y., Shackleton, R.M. & Zhang, H., 1990. The structure of 1985 Tibet Geotraverse, Lhasa to Golmud, in *The Geological Evolution of the Qinghai-Tibet,* pp. 321–347, ed. Sino-British Comprehensive Geological Expedition Team of the Qinghai-Tibet Plateau, Science Press, Beijing (in Chinese).

Deamer, G.A. & Kodama, K.P., 1990. Compaction-induced inclination shallowing in synthetic and natural clay-rich sediments, *J. geophys. Res.,* **95,** 4511–4530.

Dewey, J.F., Shackleton, R.M., Chang, C.F. & Sun, Y.Y., 1990. The tectonic evolution of the Tibetan plateau, in *The Geological Evolution of the Qinghai-Tibet,* pp. 384–415, ed. Sino-British Comprehensive Geological Expedition Team of the Qinghai-Tibet Plateau, Science Press, Beijing (in Chinese).

Dickinson, W.R. & Butler, R.F., 1998. Coastal and Baja California paleomagnetism reconsidered, *Geol. Soc. Am. Bull.,* **110,** 1268–1280.

Fisher, R.A., 1953. Dispersion on a sphere, *Proc. R. Soc. London A,* **217,** 295–305.

Frost, G.F. *et al.*, 1995. Cretaceous paleomagnetic results from the Gansu Corridor, China, *Earth planet. Sci. Lett.,* **129,** 217–232.

Gilder, S., Zhao, X., Coe, R., Meng, Z.F., Courtillot, V. & Besse, J., 1996. Paleomagnetism, tectonics and geology of the Southern Tarim Basin, Northwestern China, *J. geophys. Res.,* **101,** 22 015–22 032.

Gilder, S. *et al.*, 1999. Tectonic evolution of the Tancheng-Lujiang (Tan-Lu) fault via Middle Triassic to Early Cenozoic paleomagnetic data, *J. geophys. Res.,* **104,** 15 365–15 390.

Gilder, S., Chen, Y. & Sen, S., 2001. Oligo-Miocene magnetostratigraphy and rock magnetism of the Xishuigou section, Subei (Gansu Province, western China) and implications for shallow inclinations in central Asia, *J. geophys. Res.,* **106,** 30 505–30 521.

Halim, N. *et al.*, 1998. New Cretaceous and Early Tertiary paleomagnetic results from Xining-Lanzhou basin, Kunlun and Qiangtang blocks, China: implications on the geodynamic evolution of Asia, *J. geophys., Res.,* **103,** 21 025–21 045.

Harland, W.B., Armstrong, R.L., Cox, A.V., Craig, L.E., Smith, A.G. & Smith, D.G., 1990. A geologic time scale 1989, pp. 1–263, Cambridge University Press, Cambridge.

Harrison, T.M., Yin, A. & Ryerson, F.J., 1998. Orographic evolution of the Himalaya and Tibet, in *Tectonic Boundary Conditions for Climate Reconstructions,* pp. 39–72, eds Crowley, T.J. & Burke, K., Oxford University Press, New York.

Huang, K.N. & Opdyke, N.D., 1992. Paleomagnetism of Cretaceous to Lower Tertiary rocks from southwestern Sichuan: a revisit, *Earth planet. Sci. Lett.,* **112,** 29–40.

IAGA Division V, Working Group 8,1995, International geomagnetic reference field, 1995 revision, *J. Geomag. Geoelectr.,* **47,** 1257–1261.

Jaeger, J.J., Courtillot, V. & Tapponnier, P., 1989. Paleontological view of the ages of the Deccan Traps, the Cretaceous/Tertiary boundary and the India–Asia collision, *Geology,* **17,** 316–319.

Kirschvink, J.L., 1980. The least-squares line and plane and the analysis of paleomagnetic data, *Geophys. J. R. astr. Soc.,* **62,** 699–718.

Kodama, K.P. & Davi, J.M., 1995. A compaction correction for the paleomagnetism of the Cretaceous Pigeon Point formation of California, *Tectonics,* **14,** 1153–1164.

Kodama, K.P. & Tan, X., 1997. Central Asian inclination anomalies: possible inclination shallowing in redbeds?, *EOS, Trans. Am. geophys. Un.,* **78,** F174.

Kutzbach, J.E., Prell, W.L. & Ruddiman, W.F., 1993. Sensitivity of Eurasian climate to surface uplift of the Tibetan plateau, *J. Geology,* **101,** 177–190.

Lin, J. & Watts, D.R., 1988. Palaeomagnetic constraints on Himalayan–Tibetan tectonic evolution, *Phil. Trans. R. Soc. Lond.,* A, **326,** 177–188.

Liu, Z. & Wang, C., 1999. Oil shale in the Tertiary Hoh Xil basin, northern Qinghai-Tibet plateau, *AAPG Bull.,* **83,** 1890.

Liu, Z., 1999. Sedimentology of the Tertiary basins in the Hinterland of the Qinghai-Tibet Plateau: applications for the plateau uplift history and mechanism using GIS, *PhD thesis*, Chengdu University of Technology, Chengdu (in Chinese with English abstract).

Liu, Z. & Wang, C., 2001. Facies analysis and depositional systems of Cenozoic sediments in the Hoh Xil basin, northern Tibet, *Sediment. Geol.,* **140,** 251–270.

McFadden, P.L., 1990. A new fold test for palaeomagnetic studies, *Geophys. J. Int.,* **103,** 163–169.

McFadden, P.L. & McElhinny, M.W., 1988. The combined analysis of remagnetiztion circles and direct observations in paleomagnetism, *Earth planet. Sci. Lett.,* **87,** 161–172.

McFadden, P.L. & McElhinny, M.W., 1990. Classification of the reversal test in palaeomagnetism, *Geophys. J. Int.,* **130,** 725–729.

Meng, Z., 1991. Paleomagnetic study of Upper Paleozoic erathem along the southwestern margin of Tarim block, China, *Acta Sedimentologica Sinica,* **9,** 105–109 (in Chinese with English abstract).

Merrill, R.T., McElhinny, M.W. & McFadden, P.L., 1996. *The Magnetic Field of the Earth: Paleomagnetism, the Core and the Deep Mantle,* Academic Press, San Diego.

Molnar, P. & Tapponnier, P., 1975. Cenozoic tectonics of Asia: effects of a continental collision, *Science,* **189,** 419–426.

Opdyke, N.D. & Channell, J.E.T., 1996. Magnetic stratigraphy, International Geophysics Series, Vol. 64, pp. 1–341, Academic Press, San Diego.

Otofuji, Y., Funahara, S., Matsuoo, J., Murata, F., Nishiyama, T., Zheng, X. & Yaskawa, K., 1989. Paleomagnetic study of western Tibet: deformation of a narrow zone along the Indus Zangbo suture zone in southern Tibet, *Earth planet. Sci. Lett.,* **107,** 369–379.

Otofuji, Y., Kadoi, J., Funahara, S., Murata, F. & Zheng, X., 1991. Paleomagnetic study of the Eocene Quxu pluton of the Gandese Belt: crustal deformation along the Indus Zangbo suture between India and Asia, *Earth planet. Sci. Lett.,* **92,** 307–316.

Patriat, P. & Achache, J., 1984. India–Eurasia collision chronology has implications for crustal shortening and driving mechanism of plates, *Nature,* **311,** 615–621.

Pozzi, J.-P. & Feinberg, H., 1991. Paleomagnetism in the Tajikistan: continental shortening of the European margin in the Pamirs during Indian Eurasian collision, *Earth planet. Sci. Lett.,* **103,** 365–378.

Rage, J.C. *et al.*, 1995. Collision age, *Nature,* **375,** 286.

Richter, F., Rowley, D.B. & DePaolo, D.J., 1992. Sr isotope evolution of seawater: the role of tectonics, *Earth planet. Sci. Lett.,* **109,** 11–23.

Ruddiman, W.F, 1998. Early uplift in Tibet?, *Nature,* **394,** 723–725.

Ruddiman, W.F. & Kutzbach, J.E., 1991. Plateau uplift and climatic change, *Scient. Am.,* **264,** 66–75.

Ruddiman, W.F., Raymo, M.E., Prell, W.L. & Kutzbach, J.E., 1997. The uplift-climate connection: a synthesis, in *Tectonic Uplift and Climate Change,* pp. 471–515, ed.Ruddiman, W.F., Plenum Press, New York.

Rumelhart, P.E., Yin, A., Cowgill, E., Butler, R., Zhang, Q. & Wang, X., 1999. Cenozoic vertical-axis rotation of the Altyn Tagh fault system, *Geology,* **27,** 819–822.

Smethurst, M.A., Khramov, A.N. & Torsvik, T.H., 1998. The Neoproterozoic and Palaeozoic palaeomagnetic data for the Siberian platform: from Rodinia to Pangea, *Earth Sci. Rev.,* **43,** 1–24.

Tan, X.T. & Kodama, K.P., 1998. Compaction-corrected inclinations from southern California Cretaceous marine sedimentary rocks indicate no paleolatitudinal offset for the Peninsular Ranges terrane, *J. geophys. Res.,* **103,** 27 169–27 192.

Tan, X.T., Kodama, K.P. & Fang, D., 1996. A preliminary study of the effect of compaction on the inclination of redeposited hematite-bearing sediments disaggregated from Eocene redbeds (Suweiyi Fm) from the Tarim Basin, Northwest China, AGU 1996 Fall Meeting, *EOS, Trans. Am. geophys. Un.,* **77,** 155.

Tapponnier, P., Mattauer, M., Proust, F. & Cassaigneau, C., 1981. Mesozoic ophiolites, sutures and large scale Tetonic movements in Afghanistan, *Earth planet. Sci. Lett.,* **97,** 355–371.

Tapponnier, P., Xu, Z.Q., Roger, F., Meyer, B., Arnaud, N., Wittlinger, G. & Yang, J.S., 2001. Oblique stepwise rise and growth of the Tibet plateau, *Science,* **294,** 1671–1677.

Tauxe, L. & Kent, D.V., 1984. Properties of a detrital remanence carried by hematite from study of modern river deposits and laboratory redeposition experiments, *Geophys. J. R. astr. Soc.,* **77,** 543–561.

Tauxe, L., Mullender, T.A.T. & Pick, T., 1996. Pot-bellies, wasp-waists and superparamagentism in magnetic hysteresis, *J. geophys. Res.,* **101,** 571–583.

Thomas, J.C., Perroud, H., Cobbold, P.R., Bazhenov, M.L., Burtman, V.S., Chauvin, A. & Sadybakasov, E., 1993. A paleomagnetic study of Tertiary formations from the Kyrgyz Tien-Shan and its tectonic implications, *J. geophys. Res.,* **98,** 9571–9589.

Thomas, J.C., Chauvin, A., Gapais, D., Bazhenov, M.L., Perroud, H., Cobbold, P.R. & Burtman, V.S., 1994. Paleomagnetic evidence for Cenozoic block rotations in the Tadjik depression (Central Asia), *J. geophys. Res.,* 15 141–15 160.

Van der Voo, R., 1993. Paleomagnetism of the Atlantic, Tethys and Iapetus Oceans, pp. 1–411, Cambridge University Press, Cambridge.

Wang, C., Liu, Z., Zhao, X. & Liu, S., 1999. Sedimentology of the Fenghuoshan Group in the Hoh Xil basin, northern Qinghai-Tibet plateau: implication for the plateau uplift history, The 14th Himalaya–Karakorum–Tibet Workshop Abstracts, *Terra Nostra,* **99,** 166–167.

Westphal, M., 1993. Did a large departure from the geocentric axial dipole hypothesis occur during the Eocene?: evidence from the magnetic polar wander path of Eurasia, *Earth planet. Sci. Lett.,* **117,** 15–28.

Yi, J., Xu, J., Liu, C. & Li, H., 1990. The Tibetan plateau: regional stratigraphic context and previous work, in *The Geological Evolution of the Qinghai-Tibet,* pp. 1–48, ed. Sino-British Comprehensive Geological Expedition Team of the Qinghai-Tibet Plateau, Science Press, Beijing (in Chinese).

Yin, A. & Harrison, T.M., 2000. Geologic Evolution of the Himalayan–Tibetan Orogen, *Annu. Rev. Earth Planet. Sci.,* **28,** 211–280.

Zhang, Y. & Zheng, J., 1994. *Geological survey of the Hoh Xil and adjacent regions in Qinghai province,* pp. 1–177, Seismological Press, Beijing (in Chinese and English abstract).

Zhao, X., Coe, R.S., Zhou, Y., Hu, S., Wu, H., Kuang, G., Dong, Z. & Wang, J., 1994. Tertiary paleomagnetism of North and South China and a reappraisal of Late Mesozoic paleomagnetic data from Eurasia: implications for the Cenozoic tectonic history of Asia, *Tectonophysics,* **235,** 181–203.

Zhao, X., Coe, R.S., Gilder, S.A. & Frost, G.M., 1996. Palaeomagnetic constraints on the palaeogeography of China: implications for Gondwanaland, *Australian J. Earth Sci.,* **43,** 643–672.

Zhao, X. *et al.*, 2001. Preliminary paleomagnetic results from Cretaceous basalts of the Trans-Baikal Region, Southeastern Siberia, *EOS, Trans. Am. geophys. Un.,* **82,** Fall Meeting Suppl., San Francisco, F314.

Zhao, X. *et al.*, 2002. Paleomagnetic results from Cretaceous and Tertiary basalts of the Trans-Baikal region, southeastern Siberia, EGS XXVII General Assembly, Nice, France, April 2002, Geophysical Research Abstracts, Vol. 4.

Zijderveld, J.D.A., 1967. A.C. demagnetization of rocks: analysis of results, in *Methods in Palaeomagnetism,* pp. 254–286, edsCollision, D.W., Creer, K.M. & Runcorn, S.K., Elsevier, New York.